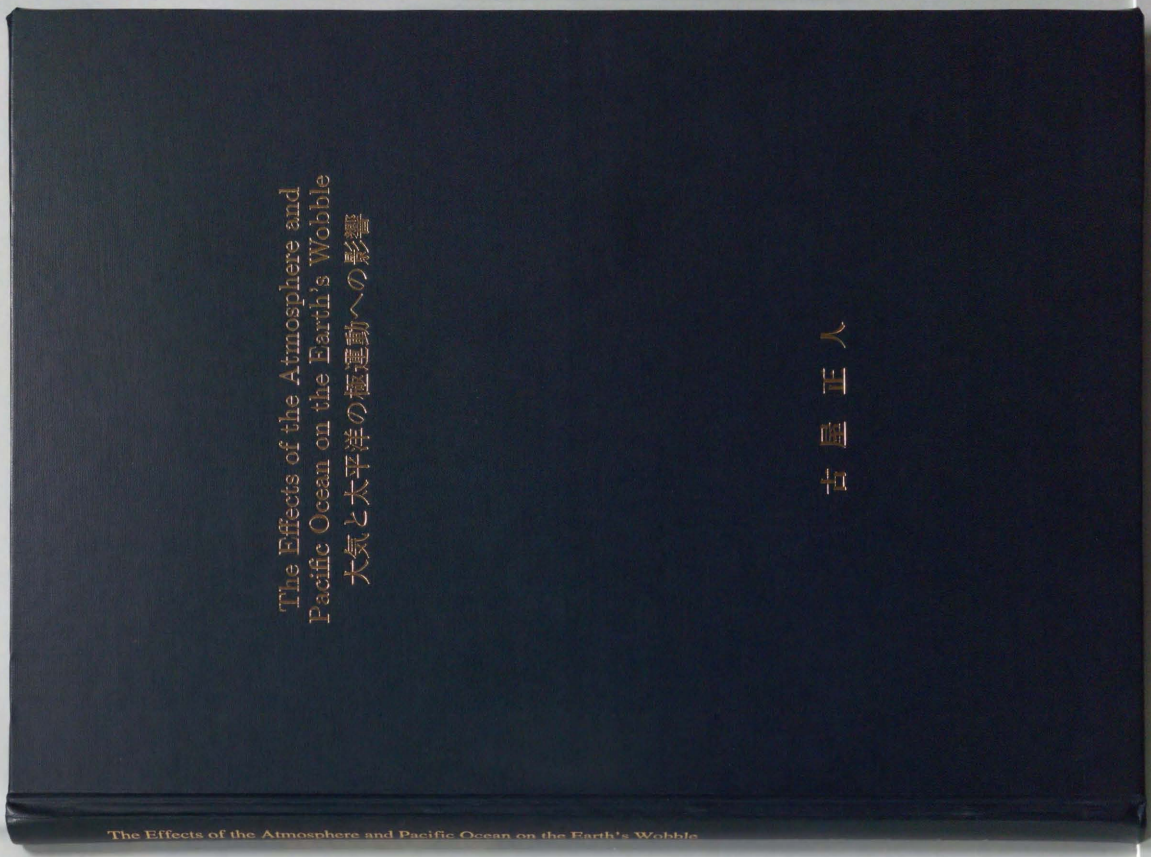
The Effects of the Atmosphere and
Pacific Ocean on the Earth's Wobble
大気と太平洋の極運動への影響
吉里正人
The Effects of the Atmosphere and Pacific Ocean on the Earth's Wobble

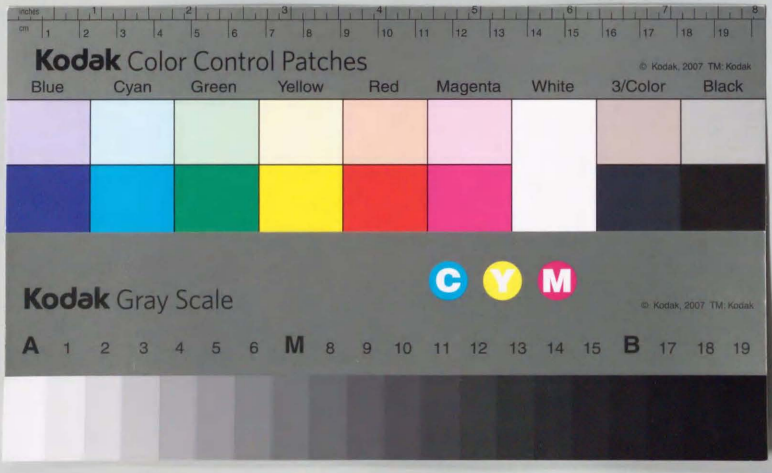
Kodak Color Control Patches
© Kodak, 2007 TM: Kodak
Blue
Cyan
Green
Yellow
Red
Magenta
White
3/Color
Black
Kodak Gray Scale
© Kodak, 2007 TM: Kodak
A 1 2 3 4 5 6 M 8 9 10 11 12 13 14 15 B 17 18 19

学位論文

The Effects of the Atmosphere and Pacific Ocean on the Earth's Wobble

大気と太平洋の極運動への影響

平成８年１２月博士(理学)申請

東京大学大学院理学系研究科

地球惑星物理学専攻

古屋　正人

Ph.D Thesis

The Effects of the Atmosphere and Pacific Ocean on the Earth's Wobble

Masato Furuya
Department of Earth & Planetary Physics
Graduate School of Science, University of Tokyo
December 1996

ISBN 9–99–999999–9 Printed in Japan

Contents

List of Figures

Preface

In this thesis, an up-to-date understanding on the excitation source(s) of the Earth's wobble is presented, which is provided by employing novel data sets; the SPACE95 is used for Earth's wobble, and the atmospheric angular momentum (AAM) are computed based on the global reanalysis data from U. S. National Center for Environmental Prediction (NCEP). We also employed the Pacific Ocean analysis data available from NCEP.

Readers who do not have time to go through the whole texts can skip both Chapter 1 and 2, in which reviews of previous understanding on wobble excitation are given. Though the review of former works is important in its own right, this can be enabled by that from Chapter 3 on, I provided a brief introduction in every chapter. However, I also included a shorter preview on the subject which will not necessarily appear in subsequent Chapters. Listed below is a brief and qualitative summary of my analysis in later Chapters:

For seasonal wobble excitation,

- Although it explains the χ_2 very well, the AAM hardly contributes to the χ_1 (Chapter 3).
- For atmospheric seasonal wobble excitation, the air pressure fluctuation near Himalayas range is truly important, but that around Tibetan plateau varies rather out of phase with the total contribution (Chapter 3).
- The Pacific Ocean contribution can well account for the χ_1, and its influence on the χ_2 is small. Thus, much of the seasonal wobble excitation could be explained (Chapter 4).
- The atmosphere and Pacific Ocean contribute via the fluctuation of moment of inertia and relative angular momentum, respectively (Chapter 3 and 4).
- The seasonal fluctuation of Pacific Ocean current contribution localizes very much around western Pacific region. In particular, the variability right south of Taiwan and east of Philippine is most intensive (Chapter 4).

For atmospheric and Pacific Ocean Chandler wobble excitation,

- The NCEP atmospheric contribution does not fully account for the Chandler wobble (Chapter 5).
- Comparing the relative importance of pressure and wind effect, the wind term plays a more significant role than the pressure term (Chapter 5).
- Intercomparison of NCEP AAM with JMA AAM assures the insignificant effect of atmospheric pressure term for Chandler wobble excitation, while the accuracy of non-seasonal wind term remains uncertain (Chapter 5).
- The larger effect of Pacific Ocean than the global atmospheric effect indicates a potential importance for the oceanic excitation of Chandler wobble (Chapter 6).

Moreover, two short notes are presented in Appendix A and B. Either of the appendices has been arranged during my visit to NASA/GSFC. To my knowledge, it has never been argued that the damping term in the conventional polar motion equation does *not* represent a Newtonian damping. I explicitly illustrate how the conventional equation will be altered when a Newtonian damping is assumed. Appendix B is cited in *Furuya and Chao* [1996].

Acknowledgment

This thesis is indebted to many people for their help, advice, encouragement and support. I should thank Prof. Yozo Hamano, my supervisor, for his insightful advice and comment on the results; the study has been greatly improved by many lengthy discussions. I should also acknowledge Prof. Isao Naito at National Astronomical Observatory, Mizusawa. He gave me much useful and up-to-date information on the Earth rotation studies, which undoubtedly led me so smoothly into this area; his encouragements were indispensable for my study. Moreover, owing to Prof. Naito, I could keep in touch with Dr. Benjamin Fong Chao, at National Aeronautics and Space Administration/Goddard Space Flight Center. I thank Dr. Chao very much for providing me a chance to work together at GSFC from July to December in 1995. Through that time, I could learn what is indispensable as an active researcher.

Dr. Richard S. Gross at Jet Propulsion Laboratory, is thanked for his un-selfishly presenting the polar motion data to the public. I thank the Numerical Prediction Division of the Japan Meteorological Agency for providing us the JMA data, and also appreciate Dr. Chi Fan Shih at National Center of Atmospheric Research, USA for his preparation of NCEP reanalysis data. Dr. Roland Schweitzer at Climate Diagnostics Center/NOAA/ERL, USA is appreciated for preparing and sending the NCEP ocean analysis data. I am grateful to Mr. Takashi Kagimoto, one of my classmates for kindly responding my inquiries about physical oceanography as well as letting me use the output of his study; the preliminary experiment based on the output data undoubtedly helped to accelerate subsequent works. Other than those I mentioned here, I also thank many colleagues and staffs in our department.

I should express my gratitude to Naoko Furuya, my wife, for her continual encouragement and house-keeping, without which I could not have accomplished this work.

Part I

Introduction –Review and Preview–

Chapter 1

Annual Wobble

1.1 Seasonal Variability in Earth Rotation

The Earth's angular velocity vector varies over a broad range of time scales for both its amplitude and orientation. The fluctuation of amplitude, i.e., angular velocity itself, is observed as length of day change, while that of orientation relative to the terrestrial reference frame is polar motion (or wobble)[1] (Figure 1.1). These Earth rotation variations are the consequences of angular momentum conservation of variety of Earth's subsystem, such as atmosphere, ocean, hydrosphere, lithosphere (mantle) and core.

The pronounced seasonal variations in the Earth's wobble are undoubtedly maintained by fluctuations in atmosphere, ocean and land water (i.e., water remaining on land and not flowing out to ocean). However, it has not been quantitatively explained yet [e.g., *Chao and Au*, 1991; *King and Agnew*, 1991], despite that the seasonal fluctuation of length of day can be well explained only in terms of axial component of atmospheric angular momentum (AAM) [e.g., *Hide and Dickey*, 1991; *Rosen*, 1993].

Since the seasonal wobble is a consequence of seasonal angular momentum fluctuation

[1]The rapid polar motion with higher frequencies around 1 cycle per day corresponds to the so-called precession and nutation

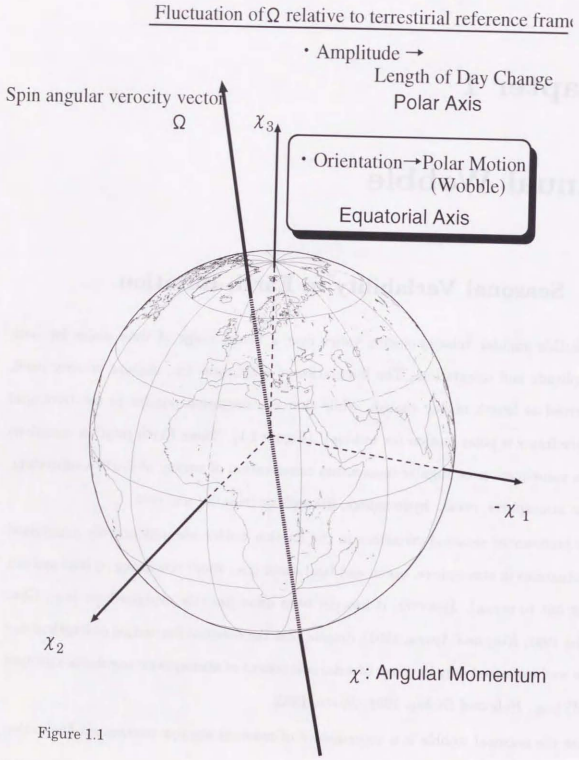

Figure 1.1

around equatorial axes, by examining its excitation budget, we can shed light on the meridional angular momentum transfer within the Earth's subsystems. This would be of importance for atmospheric general circulation, since the angular momentum fluctuation around equatorial axes is indispensable to maintain the zonal wind structure; it will also involve other geophysical disciplines, such as physical oceanography and hydrology (and possibly seismology [see, *Oort*, 1989]). Furthermore, it would be a reasonable strategy to assess the seasonal wobble excitation, whose excitation amplitude will be larger than that of the elusive Chandler wobble excitation.

1.2 Prograde and Retrograde Decomposition

Though the angular momentum fluctuation for both the atmosphere and ocean will probably have semi-annual and other higher harmonic components as well as annual component, the annual variation has been unequivocally observed as the seasonal wobble since the discovery of Chandler wobble. The standing-out of annual wobble is not only because the forcing amplitude is large, but also because the annual wobble is considered to be amplified by its proximity to the Chandler resonant frequency, about 0.86 cycle per year[2]. For the latter reason, the prograde excitation of annual wobble would be more accurately determined than the retrograde component; this argument appears to be given by *Jeffreys* [see the footnote in pp. 94 of *Munk and MacDonald*, 1960]. Thus, the previous works on annual wobble excitation has been examined, after decomposing expressly the original two forcing components into prograde and retrograde components [e.g., *Wilson and Haubrich*, 1976; *Merriam*, 1982; *Wahr*, 1983; *Chao and Au*, 1991; *King and Agnew*, 1991].

Employing several independently obtained space-geodetic data, *King and Agnew* [1991] examined the prograde and retrograde annual wobble excitation, and intercompared each

[2]This latter idea is based on the assumption that the Earth's resonant wobbling frequency is unique and stable, on which we will also rely in this study

space-geodetic results with that inferred from the International Latitude Service (ILS) data. As a result, it was found that the the retrograde annual excitation determined in ILS data is much larger than that in newer data, while the prograde excitation in ILS data is consistent with that in newer data. Thus, they suggested that the retrograde component in older data was certainly corrupted by some systematic noise.

Unfortunately, however, *King and Agnew* [1991] did not place their emphasis on the consistency of newly determined retrograde excitations which assures the quality of three different space-geodetic data sets. We consider that the result has an important implication. As stated above, the original motief of pro- and retrograde decomposion is to reject the retrograde excitation corrupted by noise; for instance, *Chao and Au* [1991] did not illustrate the result for retrograde annual excitation. However, now that the space-geodetically observed data have turned out to detect even the retrograde excitation with sufficient quality as well as the prograde component, we think that the conventional decomposition technique is unnecessary; we do not state that it is a wrong procedure. By doing so, we can treat the whole ingredients of angular momentum variation, in contrast with the former studies in which a part of signals have been rejected. Moreover, we can examine the seasonal wobble excitation in more intuitive manner than decomposing into pro- and retrograde component.

In subsequent sections, I will briefly review the previous studies of surfacial seasonal variability on the excitation of seasonal wobble; a more extensive review is provided by e.g., *Lambeck* [1980] and *Eubanks* [1993]. A shorter preview is also discussed for the following chapters as well as for future prospects.

1.3 Atmosphere

In general, the angular momentum fluctuation can be decomposed into mass redistribution effect and the fluctuation of relative angular momentum, as can be seen from the definition

of angular momentum, H, in rotating coordinate system with angular velocity, Ω,

$$H = \int \rho r \times (\Omega \times r + v) dV, \tag{1.1}$$

where the each term in the r. h. s. of eq. (1.1) represents, in order, the mass reditribution and the relative angular momentum (with respect to the rotating coordinate). Here ρ and r are density of the medium and position vector, respectively; the integrarion is performed over the whole volume, V.

For the atmospheric angular momentum(AAM), *Barnes et al.* [1983] have provided an elegant formulation which conforms to the available data set, surface pressure (P_s), eastward and northward wind verocity (u and v):

$$\tilde{\chi}^P = -\frac{R^4}{(C-A)g} \int\int P_s \sin\phi \cos^2\phi \exp(i\lambda) d\phi d\lambda, \tag{1.2}$$

$$\tilde{\chi}^W = -\frac{R^3}{(C-A)\Omega g} \int\int\int (u \sin\phi + iv) \exp(i\lambda) \cos\phi d\phi d\lambda dp. \tag{1.3}$$

Here, R, g, and Ω are the Earth's mean radius, mean surface gravity, and mean angular velocity, respectively; C and A are the Earth's polar and equatorial moments of inertia. The integration in eq. (1.2) is performed over latitude ϕ and longitude λ, while that in eq. (1.3) also includes the vertical integartion along the pressure coordinate.

The $\tilde{\chi}^P$ and $\tilde{\chi}^W$ represent the effect of air mass redistribution and relative angular momentum fluctuation, respectively (For details, see Chaper 3). Since the global wind data was not available in the past, the air mass redistribution effect has been extensively investigated; this is also partly because the wind contribution was at one time errorneously thought to be negligible, but corrected by *Barnes et al.* [1983] and *Wahr* [1983].

1.3.1 Air Mass

The study on the effect of seasonal air mass migration upon the Earth's wobble has been commenced by *Spitalor* in 1901 which is ten years after the discovery of Chandler wobble. Those who have interests in the former studies prior to 1970s should look into Chapter 9

of *Munk and MacDonald* [1960]. It should be noted that *Spitalor* had already pointed out the importance of air mass shift associated with the high pressure in winter over Siberia. However, this conclusion would be largely speculative on account of sparse distribution of atmospheric data in those days. We note that the polarized seasonal excitation inferred from annual wobble observation enables one to speculate the excitation source (see, Fig. 9.1 in *Munk and MacDonald* [1960]).

As the atmospheric data set improves in its spatial coverage, quality as well as time span, numerous authors have revisited the atmospheric mass redistribution effect on the annual wobble [e.g., *Munk and Hassan*, 1961; *Wilson and Haubrich*, 1976; *Merriam*, 1982; *Wahr*, 1983]. In evaluating this contribution, the response of ocean to overlying atmosphere must be properly treated, because, if we substituted surface pressure over ocean directly into eq. (1.2), the sea surface would be treated as rigid body. The other extreme response is called inverted barometer response [e.g, *Munk and MacDonald*, 1960; *Gill*, 1982], in which one millbar increase in local atmospheric pressure isostatically depresses the ocean surface by one centimeter. Obviously, the global air pressure fluctuation can be much reduced through this inverted barometer response [*Merriam*, 1982; *Wahr*, 1982]. The recent studies suggest the validity of inverted barometer rule at frequencies much lower than one cycle per day [e.g., *Dickman*, 1988; *Trupin and Wahr*, 1990; *Ponte*, 1994]. Thus, the atmospheric mass redistribution effect discribed in this study is based on the inverted barometer assumtion.

Nowadays, owing to the advent of four-dimensional data assimilation (4DDA) system, the global atmospheric data sets are available, in which both the surface air pressure and wind velocity at multiple levels are included with uniform spatial coverage over the globe as well as short sampling interval(four times daily at present). *Vondrák and Pejović* [1988] and *Chao and Au* [1991] examined the seasonal variation of AAM, employing 4DDA data from U. S. National Meteorological Center (NMC) and European Center for Medium range Weather Forecast (ECMWF) data, respectively; the U. S. NMC has recently been renamed

as National Center for Environmental Prediction (NCEP). Both agencies' results for pressure contribution are consistent with each other, which suggests a reliability of pressure term. Comparing this estimate with the older one [e.g., *Wahr*, 1983], both the amplitude and phase are largely the same, but the amplitude of older estimate is about 20–30 % larger than the estimate based on 4DDA data set. According to their results, the pressure term turned out to be larger than the required amplitude inferred from wobble data, especially for retrograde annual wobble. Moreover, it leaves significant phase difference from the excitation inferred from wobble data (see, Figure. 2 in *King and Agnew* [1991]).

As noted in previous section, we claim that these understandings based on the prograde and retrograde decomposition are less intuitive. We will discuss the atmospheric influence on the seasonal wobble excitation viewed from the original two forcings in Chapter 3.

1.3.2 Wind

Prior to the development of 4DDA system, the wind contribution to seasonal wobble excitation has been neglected, partly because the torque associated with geostrophic wind were shown to be zero [*Munk and MacDonald*, 1960]. The more plausible reason is, however, that the effort to estimate it had been hamperred by the lack of uniformly distributed data. Thus, *Wahr* [1982] developped a hybrid method to estimate the air motion effect [*Wahr*, 1983], in which the angular momentum is used where the velocity data are available, while the torque approach is also applied where they are sparse (see, Chapter 4).

Direct estimation of the wind term for equatorial AAM has just begun over the past decade owing to the implement of global atmospheric analysis data. Comparing the newer wind contribution with the older estimate, the difference is appreciable (Fig. 2 in *King and Agnew*, 1991). However, even today, we should note that, in contrast with the pressure term, the wind terms computed from each agency in the world are not in good agreement with each other, particulary for higher frequency variations [*Eubanks et al.* 1988; *Chao*

and Au, 1991; *Furuya et al.* 1996]. The difficulty is presumably caused by small and noisy meridional wind velocity, v, in eq. (1.3), which is still thought to be unreliable at present. Nevertheless, as far as the seasonal variation is concerned, there is no significant difference which is depicted in Figure 3.1.

Chao and Au [1991] and *Kikuchi and Naito* [1992] indicated a non-negligible role of wind contribution to the annual wobble excitation. According to *Chao and Au* [1991], the atmospheric $\tilde{\chi}^W$ has a prograde annual cycle whose amplitude is about 20 % of the pressure term. This amplitude amounts about twice that of land water excitation of prograde annual wobble estimated by *Chao and O'Connor* [1988].

Thus, owing to the 4DDA data, the wind contribution appears to be vitalized today. However, when viewed from original two coordinate axes, we recognize that the wind contribution is much smaller than the pressure contribution. Rather, we think that the true importance of atmospheric wind cannot be appreciated until we will assess the ocean current contribution. In Chapter 4, we will indicate that the Pacific Ocean current can well account for the seasonal wobble excitation which the AAM could not, and that the driving force of seasonal current fluctuation is the sea surface wind stress.

1.4 Land Water

By the term, land water, we mean continental surface water storage, i.e., precipitation (snow and rain), evapotranspiration and run-off water remaining over the land. Although we need to evaluate underground water migration which will be another potentially important source, there is no substantial observation of ground water storage at present. Thus, we will ignore it just for simplicity.

The fundamental equation for hydrological budget is given by surface water storage, Δh,

$$\Delta h = p - e - r, \tag{1.4}$$

as a function of time and location; here, p is the precipitation (snow and rain), e the evapotranspiration, and r the run-off. These quantities are usually expressed as an equivalent depth of liquid water. In general, the land water storage, Δh, can be well approximated as,

$$\Delta h \simeq \Delta W + \Delta S, \tag{1.5}$$

where ΔW and ΔS represent fluctuations of soil moisture and snow load. Multiplying the eq. (1.4) by density, ρ, leads to the surface water mass at the location. Hence, we get the following equation to estimate the surface water contribution to wobble excitation [e.g., *Chao and O'Connor*, 1988],

$$\tilde{\chi}^{LW} = -\frac{R^4\rho}{(C-A)g}\int\int[h(\phi,\lambda,t) - \bar{h}(\phi,\lambda)]\,\sin\phi\,\cos^2\phi\,\exp(i\lambda)d\phi d\lambda, \tag{1.6}$$

where the $\bar{h}(\phi,\lambda)$ is the annual avarage of equivalent water depth. Thus, land water fluctuation in eq. (1.6) contributes to the mass term in eq. (1.1).

At one time the prograde annual excitation appeared to be largely closed when *Van Hylckama* [1970]'s land water estimates are added to the atmospheric pressure contribution. However, *Chao and O'Connor* [1988] reopened the problem, paying prudent attention to the accuracy of employed data set. They explicitly pointed out a double cancellation mechanism which can induce a serious error in the excitation estimate. The mechanism is caused by spatial dependence of wobble excitation, i.e., the out of phase effect from eastern and western hemisphere in northern hemisphere, as well as seasonal polarity; in Eurasian winter there is much snow, while the Eurasian summer is monsoon season. Their optimal estimate is obtained by combining *Willmott et al.* s data set of soil moisture with the snow load contribution by *Chao et al.* [*Willmott et al.* 1985; *Chao et al.* 1987] (see eq. (1.5)). *Kuehne and Willson* [1991] also examined the land water contribution, using 612 basin global model forced by monthly mean precipitation estimates. Although the results of these newer two studies are not necessarily consistent with each other (probably owing to unknown errors of data sets), their estimates for the seasonal wobble excitation are less than 30 % of the amplitude given by *Van Hylckama* [1970].

Thus, the land water contribution are thought to be small nowadays, but the global hydrological budget itself is far from established. So that, we should note that land water influence on the wobble excitation is subject to increase its amplitude in the future. The importance of land water hydrological processes are widely recognized in climatology. For instance, the global soil moisture data set is indispensable as initial values for atmospheric global circulation and numerical weather prediction model. Such climatological data set, i.e., the mean seasonal cycle, has been obtained by *Willmott et al.* [1985] and *Mintz and Serafini* [1992]. However, *Matsuyama* [1996] argues that the soil-wetness data by *Mintz and Serafini* [1992] do not represent a water storage as both rivers and snow load. Further, the study to obtain year-to-year soil moisture variation has recently begun [*Nishimura and Sato*, 1996].

In the meantime, it is to be noted that, in attempting to examine the land water effect, only the moment of inertia fluctuation is taken into account; consider, for instance, that the perpetual snow flows and contribute to the relative angular momentum. We point out that the spatial derivarives of $h(\phi, \lambda, t)$ would be the motion term of land water which corresponds to atmospheric wind or ocean current, since it will induce a shear stress on the Earth; the mass redistribution effect corresponds to a vertical stress. To my knowledge, this point has never been estimated nor pointed out. We realized the land water 'flow' contribution in analogy with the angular momentum and torque approach in the evaluation of atmospheric wobble excitation. Surely, the land water 'flow' will be very slow, and thus might contribute to the Earth's rotational and gravitation variation with longer time scale.

1.5 Ocean

There are, to my knowledge, only a few papers, in which oceanic influence upon the Earth's annual wobble excitation is examined [*Munk and Groves*, 1952; *Wilson and Haubrich*, 1976; *O'Connor*, 1980; *Wahr*, 1983]; obviously, the lack of realistic global ocean data hampered

reliable estimate of oceanic effect.

Munk and Groves [1952] estimated the effect of ocean currents on annual wobble excitation, based on the vertically integrated mass transport stream function which had been analytically obtained in the Munk's theory on western boundary currents [*Munk*, 1950]. They states, "the circulation in the Pacific Ocean alone accounts for 10 per cent of the magnitude...". In those days, however, the observation for the seasonal transport variation is hardly available, on which their estimate rely. Thus, *Munk and MacDonald* [1960], and reiterated by *Wilson and Haubrich* [1976], stated that the effect of wind-stressed non-isostatic sea level change on the wobble excitation is the remaining question.

O'Connor [1980], based on the linearized one–layer barotropic model with flat-bottom ocean, analytically estimated the effects of wind-driven perturbation in bottom pressure on the annual excitation. He did not consider the effects of wind-driven currents. *Wahr* [1983] also employed a simple linear ocean model, i.e., the so-called Sverdrup balance with realistic ocean–continent distribution. This model was driven by the sea-surface wind stress climate values [*Hellerman and Rosenstein*, 1983]. Wahr's estimate in based on the flat-bottom barotropic model with the uniform depth of 4000m: all frictional, inertial and advective terms are ignored. Results suggested that the wind-driven ocean has little effects on the annual excitation.

Wahr [1983] gave a caveat on his results, in that the influence of two omissions of both bottom topography and density stratification is not appreciated. As he stated, bottom topography can potentially contribute to a mountain-torque between the ocean and solid Earth [this idea was pioneered by *Munk and Palmen*, 1951]. However, he considered that the most prominent 'mountains' are the ocean–continent boundaries, and that the omission might not be too serious a problem. In other words, *Wahr* [1983] examined a torque acting at precipice of 4000 m high between the ocean and solid-Earth, and neglected the baroclinicity as well as the bottom topography. In the literature of physical oceanography, it still remains unsolved questions how topography affects the ocean flow above, since it

is almost impossible to directly measure bottom pressure and thus to confirm the idea [e.g., *Holland*, 1973; *Hughes and Killworth*, 1995].

Recently, the numerical modeling of ocean general circulation has grown explosively, owing to the improvement of understanding the ocean dynamics and the advent of high performance computing facility [see, e.g., *McWilliams*, 1996]. The output data from the *Semtner and Chervin* [1992] (and its modification to the free surface model) model have been employed to assess the oceanic effect on the wobble excitation [e.g., *Steinberg et al.* 1995; *Salstein et al.* 1995] and length of day (lod) change [*Ponte and Rosen*, 1994]; *Bryan* [1995] (unpublished manuscript) also examined the oceanic influence on the length of day change, based on the Geophysical Fluid Dynamics Laboratory Modular Ocean Model. Still, it should be noted that these model output data are the output of 'simulation', and may not be compared with real-time Earth-orientation or lod data. The largest defect in these output data is that the model is driven by atmospheric climate values, and not coupled with the atmosphere above: the atmosphere–ocean interaction is not taken into account.

The ocean data assimilation, as has been done for atmosphere, is presently an active research area in physical oceanography as evidenced by the growing literature, but still in the infancy due, largely, to the lack of observation. Nevertheless, the basin-scale analyses (the Pacific and Atlantic) are presently being done at NCEP [*Leetmaa and Ji*, 1989; *Ji et al.* 1994; *Ji et al.* 1995]: the analysis data set of the Pacific Ocean is presently archived at Climate Diagnostics Center, NOAA (Anonymous ftp at ftp.cdc.noaa.gov:Datasets/leetmaa). We apply the data set in order to evaluate the Pacific Ocean contribution to the excitation of Earth's wobble, and find its pronounced influence (Chapter 4 and 6).

Chapter 2

Chandler Wobble

2.1 A Long-standing Issue

Ever since the discovery of Chandler wobble in 1891, which is the Earth's Eulerian free nutation, its amplitude has never shrunk to zero. Hence, it must have been maintained by some source(s) with some mechanism(s). However, the source(s) which excite the Chandler wobble have remained elusive (see, for a thorough review of previous studies on the excitations, *Lambeck*, 1980; *Runcorn et al.*, 1990; *Eubanks*, 1993; *Wilson*, 1993). The seismic excitation power [e.g., *Smilie and Mansinha*, 1968; *O'Connell and Dziewonski*, 1976] is found out to be too small [e.g., *Kanamori*, 1977; *Chao and Gross*, 1987; *Chao et al.*, 1996], despite a remakable correlation between the wobble amplitude and global seismicity [*Myerson*, 1970; *Kanamori*, 1977]. As to the effect of core-mantle coupling torque [e.g., *Hinderer et al.*, 1987], there's little observational evidence to support the hypothesis. Contributions from the atmosphere [e.g., *Wilson and Haubrich*, 1976; *Wahr*, 1983] and the hydrosphere [*Hinnov and Wilson*, 1987] have also been discussed. The conclusion of *Wilson and Haubrich* [1976] and *Wahr* [1983] is that the atmospheric contribution amounts up to about 20 to 30 % of the necessary variance. We should note, however, that, only a few decades ago, the atmospheric data distribution was so sparse that they could not firmly

evaluate its contribution. *Wilson and Haubrich* [1976] did not assess the wind contribution in spite of their cautious remarks for its potential importance. In order to resolve the problem of sparse data, *Wahr* [1982] developed a hybrid approach and investigated the wind contribution, but couldn't incorporate the contribution from central Asia which should be important because of its topography [*Wahr*, 1983].

Over the past decade, atmospheric angular momentum (AAM) functions have been calculated along with operational analysis of numerical weather prediction for the global atmospheric state [*Barnes et al.* 1983]. In terms of the space–geodetically obtained precise polar motion data, *Chao* [1993] states that there is a remarkable correlation between AAM and the inferred excitation, and therefore the CW is significantly excited by the atmosphere. Moreover, *Kuehne et al.* [1993] show that in some prescribed 14 months' period about 70 % of the non–seasonal variance is explained by the effect of atmospheric mass redistribution. Thus, they conclude that the CW is excited by the atmospheric mass redistribution, i.e., atmospheric pressure variation.

The AAM fuctions consist of pressure and wind term, which represent the fluctuation of moment of inertia and relative angular momentum, respectively (see eqs. (3.2) and (3.3)). From the point of view of a torque exerted on the Earth, the pressure term corresponds to a torque acting upon the Earth's ellipticity, while the wind term consists of frictional and mountain torque [e.g., *Munk and MacDonald*, 1960; *Wahr*, 1982; *Barnes et al.* 1983]. For over a few decades, the ellipticity torque caused by atmospheric pressure variation has been thought to play a principal role in maintaining the Earth's wobble. Indeed, the pressure term dominates over the wind term in annual wobble excitation [e.g., *Chao and Au*, 1991, see also Chapter 3], and causes a significant correlation with the "rapid", intra-seasonal wobble excitation [e.g., *Eubanks et al.* 1988]. However, *Brzezinski* [1995] and *Furuya et al.* [1995; 1996] have casted an alternative source in the excitation of Chandler wobble, i.e., the dominance of atmospheric wind term. It is to be noted that these results do not contradict with those discussing the pressure term, since the wind dominance is suggested

near the Chandler eigenfrequency. *Furuya et al.* [1996] further suggested that the wind term in AAM has a spectral peak near Chandler frequency, i.e., 14 months period. At present, however, the wind AAM for wobble excitation does not appear to have a sufficient accuracy [*Furuya et al.* 1996], comparing one agency's result with the other one. Thus, it merits further attention whether or not the wind AAM can explain the Chandler wobble excitation.

Meanwhile, as stated in *Furuya et al.* [1996], the AAM does not totally account for the wobble excitation over a whole frequency band. In particular, we should note that the role of both oceanic and landwater interannual variation in exciting Chandler wobble has not yet been well appreciated, owing to the lack of observation. We will provide an evidence of potential importance veiled in ocean, by employing the NCEP Pacific Ocean analysis data (Chapter 6).

2.2 Some Personal Thoughts as Future Prospect

In this section, I am going to provide a prospect for the future study of Chandler wobble and its related field. We know that there exists ample excellent review papers and monographs dealing with Earth's variable rotation [e.g., *Munk and MacDonald*, 1960; *Lambeck*, 1980; *Eubanks*, 1993; *Wilson*, 1993; *Chao*, 1994]. Thus, I consider that, rather than attempting to thouroughly review previous works at this late time, it would be worth to express my present thoughts. However, the following argument is partially based upon *Naito* [1993; personal communication].

At the outset, let's take a look again at the Earth's polar motion observation. Setting aside the slower polar drift which is the present day true polar wander, we can see a six-year beeting phenomenon which is caused by superposing two components, i.e., annual and 1.2 year-Chandler wobble. The sources to maintain the annual wobble is obviously the seasonal variation prevailing over the ground surface, and thus the annual wobble is a result

of forced oscillation. On the other hand, soon after the Chandler wobble was discovered, *Newcomb* [1892] pointed out that the Earth's elastic yielding as well as oceanic fluidity would account for the contradicting period at that time with that based on rigid body theory. Based on the Newcomb's remark, the Chandler wobble has been considered as the Earth's free nutation period; the Chandler period is interpreted by the Earth's numerous dynamical properties [e.g., *Smith and Dahlen*, 1981; *Okubo*, 1982b].

The Newcomb's idea surely forms a basis of widely accepted polar motion equation, eq. (3.1), which asserts single and invariable eigen frequency. My personal thoughts are concerned with the classical dynamics and formulation of Chandler wobble[1]. However, before presenting my argument, we should keep in mind that there have already been some studies against the classical theory (see, for a review, e.g., *Eubanks* [1993]). At one time, there was a debate on variability of the Chandler period. *Carter* [1981] noted a variation of the Chandler period, which correlates with the wobble amplitude, and interpreted as a consequense of nonlinear pole tide; in contrast, when theoretically explaining the Chandler frequency, the pole tide has been assumed to follow the equilibrium theory [e.g., *Smith and Dahlen*, 1981; *Dickman and Steinberg*, 1986]. However, *Okubo* [1982a] indicated that, even on the assumption of single and invariable eigen frequency, a synthetic Chandler wobble excited by gaussian noise appears as if it has variable Chandler period, depending on the prescribed Q values. This study suggested that we did not have to modify the classical wobble equation even for the variable Chandler period model. Moreover, there has been reports suggesting multiple Chandler periods [e.g., *Dickman*, 1981; *Chao*, 1983]. *Eubanks* [1993] noted that, if there are multiple of periods, the Q values would have to be extraordinary high; note, however, that this remark is based upon the excitation spectrum is flat near the Chandler frequency. Still worse, there has been no physical argument compelling multiple Chandler period.

[1]Note that these ideas are derived from subsequent analyses in which I totally followed the conventional equation of motion...

Although there appears no reason to invoke an alternative model on the Chandler wobble, readers should be aware that all the foregoing studies have been based on the ILS polar motion data set which is less accurate than presently available data. Still worse, their argument relied on an imperfect knowledge on the wobble excitation; note that homogeneous global atmospheric data set has just become available over the last decade.

My personal thought comes from the analysis on the atmospheric excitation of Chandler wobble [*Furuya et al.* 1996]. Employing Japan Meteorological Agency's AAM, *Furuya et al.* [1996] suggested that the Chandler wobble is maintained by wind signal with a periodicity of about 14 months. Further, they noted that the periodic wind excitation of Chandler wobble is in harmony with the recent result on the enhanced amplitude of pole tide at North Sea; although the North Sea pole tide has been well-known for its enigmatically enhanced pole tide(14 months' tide), *Tsimplis et al.* [1994] showed that it could be explained by the periodic wind stress with 14 month's periodicity (for a review, see the references therein). Thus, we may regard both the Chandler wobble and non-equilibrium pole tide at North Sea as a response to the external forcing with its period about 14 months. Note that the Chandler wobble excitation has been frequently modeled as some random noise [e.g., *Okubo*, 1982a; *Chao*, 1985]. Thus, this idea is evidently an alternative to the previous premise. Moreover, it may upset the conventional formulation itself, which takes the form of traditional auto-regressive model with order one [e.g., *Wilson*, 1985. Also see, *Ooe*, 1978].

Although the influences of atmospheric interannual variation on length of day change have been successfully reported [e.g., *Rosen et al.*, 1984; *Chao*, 1989; *Dickey et al.*, 1992], those on the wobble has been shown to be poor [*Chao*, personal communication, 1996]. In the previous literature, however, only the two widely known phenomena, i.e., the quasi-biennial oscillation(QBO) and Southern Oscillation associated with El Niño are treated as interannual variation. Note that both the QBO and SO are zonal fluctuation near the equator, and thus will not have a strong effect on the wobble.

Aside from the two well-known interannual variabilties above, we could note a 15-16 month periodicity in variety of observations such as equatorial sea surface temprature(SST), zonal wind [e.g., *Rasmussion et al.*, 1990; *Jiang et al.*, 1995], global precipitation [*Lau and Sheu*, 1988] and Eurasian snow cover [*Yanai and Li*, 1994]. Although a physical relationship with these observation remains uncertain, a near 14 month periodicity in the wind AAM suggested by *Furuya et al.* [1996] may account for the Chandler wobble excitation, and comform to the "Devil's staircase" theory of the El Niño [*Jin et al.*, 1994; *Tziperman et al.*, 1994]; *Naito and Kikuchi* [1995] have already detected a quasi–seven months oscillation whose relation with ENSO is suggested. However, as *Furuya et al.* [1996] noted, the equatorial wind AAM appears to be corrupted by noise probably due to meridional wind, and awaits further improvement in its quality; the accuracy of meridional wind field will also be important as a proper driving force for wind-driven ocean circulation.

The other fact which has been bothering me is the sensitive dependence of inferred-excitation amplitude on the prescribed Chandler period [*Furuya et al.* 1996]. We illustrated that, when the Chandler period is assumed around 435–436 days, the excitation inferred from wobble data takes a minimun amplitude [*Furuya et al.* 1996]. At first sight, the Chandler period giving rise to the minumum appears to be a correct Chandler period, since the deconvolution filter by *Wilson* [1985] is a notch–filter rejecting a power around the specified frequency. In other words, this indicates that the wobble spectrum achieves a peak at the frequency, 0.84 cycle per year(cpy), corresponding to 435 days of period. However, it would be serious that the inferred excitation amplitude is much less than that computed from AAM excitation, since it is implausible that other sources can "skillfully" cancel the excess AAM effect; a similar result is obtained by *Brzezinski* [personal communication, 1995]. Meanwhile, we can interpret the result in the other way; the wobble spectrum has actually "no" power near the frequency around 0.84 cpy, though the data span does not allow sufficient frequency resolution in terms of conventional spectral analysis. This interpretation may revitalize the splitting feature of polar motion spectrum.

Part II

Atmosphere and Pacific Ocean Excitation of the Seasonal Wobble

Chapter 3

Atmospheric Influence

3.1 Abstract

Global atmospheric reanalysis monthly data from U. S. National Center for Environmental Prediction (NCEP) are used to compute atmospheric angular momentum (AAM) and to revisit the atmospheric influence on the Earth's seasonal wobble. Preceding the analysis, we point out that the conventional decomposition technique into pro- and retrograde components is not necessary as long as one employs high precision Earth's orientation data; thus, we compare the averaged yearly two components of torque, χ_1 and χ_2, orienting toward 90 deg. west longitude and Greenwich meridian, respectively. Although the seasonal AAM fluctuation does not totally account for the observed yearly excitation as shown previously, we indicate that the discrepancy mainly originates in the χ_1 component, which anticipates the oceanic contribution as the other potentially important source. We also examine the atmospheric regional contribution to the χ_2. It is found that the surface air pressure variation near Himalayas range is important as has been inferred from observed excitation, while that around Tibetan plateau varies rather in out-of-phase manner.

3.2 Introduction

The Earth's orientation change with respect to a terrestrial frame of reference has been observed as polar motion since the discovery of Chandler wobble in late 1800 [e.g., *Munk and MacDonald*, 1960; *Lambeck*, 1980]. The annual wobble has also been observed, and is the other largest component than Chandler wobble. Obviously, it is seasonally-forced motion because of its period. Thus, there are an ample literature discussing the effect of surface seasonal change such as atmosphere, land water and ocean etc. on its excitation (see, for a review, e.g., *Munk and MacDonald*, 1960; *Lambeck*, 1980; *Eubanks*, 1993 and the references therein). However, the budget of seasonal wobble excitation is not yet closed [e.g., *Chao and Au*, 1991; *King and Agnew*, 1991].

In this paper, we will investigate the atmospheric contribution to the Earth's annual wobble excitation, employing U. S. National Center for Environmental Prediction (NCEP) reanalysis data which have been available as of March 1996. As stated above, this problem is not a new one; the first attempt to explain it by seasonal air mass change goes back to 1901 by Spitaler. Still, we believe that it is worth to revisit the problem for the reason discussed below. The most important point is concerned with the recent significant improvement of data quality for both polar motion and global atmosphere. Though this point has been already mentioned in, for instance, *Chao and Au*, 1991, the two dimensional excitation function has still been decomposed into pro- and retrograde component. This is because the retrograde component has been less accurately determined in optically observed data[*Munk and MacDonald*, 1960, pp. 94]. However, we point out the un-necessity of the conventional technique, and thus could effectively utilize the high-quality data. By so doing, we will intuitively shed light on the discrepancy between the AAM contribution and the observed excitation. Moreover, the atmospheric regional contribution could be examined, which is enabled by homogeneous data distribution of global atmosphere; though the prominent seasonal fluctuation originating in the pressure term over Eurasian continent

has been widely recognized [e.g., *Munk and MacDonald*, 1960; *Lambeck*, 1980], the foregoing argument is largely based on a insufficiently distributed data set. Moreover, the wind term's role has not yet fully documented because equatorial wind term is known to be notoriously noisy: even for the seasonal variation, they were inconsistent from one agency's' atmospheric angular momentum (AAM) to the others' (but, see below).

3.3 Theory

The governing equation of the Earth's wobble is given by

$$\frac{i}{\tilde{\sigma}_{CW}}\frac{d\tilde{\mathbf{m}}}{dt} + \tilde{\mathbf{m}} = \tilde{\chi} - \frac{i}{\Omega}\frac{d\tilde{\chi}}{dt}, \tag{3.1}$$

where $\tilde{\mathbf{m}}$ and $\tilde{\chi}$ represent the wobble and excitation, respectively [*Munk and MacDonald*, 1960; *Lambeck*, 1980]; the $\tilde{\sigma}_{CW}$ represents complex Chandler frequency, i.e., the frequency and Q of Chandler wobble. The $\tilde{\mathbf{m}}$ and $\tilde{\chi}$ are defined as $m_1 + im_2$ and $\chi_1 + i\chi_2$, where the subscripts 1 and 2 refer to the axes in the equatorial plane along the Greenwich meridian and 90degE longitude, respectively: the variable angular velocity vector is written as $\Omega(m_1, m_2, 1 + m_3)$. The $\tilde{\chi}$ itself represents a non-dimensional angular momentum fluctuation, and thus the sum of two terms in eq. (3.1) results in the total torque exciting the wobble. However, *Gross* [1992] have provided a modern formulation which conforms to the space-geodetic Earth orientation data; the formulation is valid for a long-period approximation, and apparently, the second term in the r. h. s. of eq. (3.1) can be ignored (see also, Appendix A).

Barnes et al. [1983] have given an elegant formulation of AAM as a candidate for $\tilde{\chi}$, in which to a good approximation the AAM function can be separated into so-called pressure($\tilde{\chi}^P$) and wind($\tilde{\chi}^W$) term. They are explicitly,

$$\tilde{\chi}^P = -\frac{R^4}{(C-A)g}\int\int P_s \sin\phi \cos^2\phi \exp(i\lambda) d\phi d\lambda, \tag{3.2}$$

$$\tilde{\chi}^W = -\frac{R^3}{(C-A)\Omega g}\int\int\int (u\sin\phi + iv)\exp(i\lambda)\cos\phi d\phi d\lambda dp. \tag{3.3}$$

Here, R, g, and Ω are the Earth's mean radius, mean surface gravity, and mean angular velocity, respectively; C and A are the Earth's polar and equatorial moments of inertia; P_s is the surface air pressure; u and v are the eastward and northward velocity. The integration in eq. (3.2) is performed over latitude ϕ and longitude λ, while that in eq. (3.3) also includes the vertical integration along the pressure coordinate.

3.4 Data and Computation

The Earth's wobble data set is SPACE95 [see, *Gross*, 1996], in which a Kalman filter is used to combine independent measurements of the Earth's orientation taken by the space-geodetic techniques such as very long baseline interferometry, satellite laser ranging, lunar laser ranging and global positioning system. SPACE95 is a daily series, spanning October, 1976 to February, 1996. We deconvolved the wobble data into the excitation series, based on the Wilson's simplest filter (2a) in *Wilson*, 1985; hereafter, we call the deconvolved series inferred excitation. The prescribed period and Q of Chandler wobble are 434 days and 100, respectively [e.g., *Wilson and Vicente*, 1990; *Furuya and Chao*, 1996]. Since we subsequently employ the monthly atmospheric data, we average the daily inferred excitation into monthly series.

The AAM computation in the present paper is based on the monthly NCEP reanalysis data, of which we used ground surface pressure and east- and north-ward wind velocity data on a 2.5 deg $\times$ 2.5 deg latitude-longitude grid at 17 levels of altitude. We substituted them in eqs. (3.2 and 3.3). The series spans from January, 1979 to December, 1995 [*Kalnay et al.* 1996].

In order to properly evaluate the atmospheric influence upon the Earth's wobble excitation, we have to consider the response of the ocean to overlying atmospheric motion. In the previous literature, the oceanic surface response to atmospheric pressure variation has been intensively appreciated [e.g., *Merriam*, 1982; *Wahr*, 1983], while that to the shear

stress caused by atmospheric wind is largely unknown probably because the wind effect itself was considered to be small. Two idealistic behaviors are assumed in evaluating $\tilde{\chi}^P$. If the oceanic surface responds isostatically, the mass redistribution effect would be significantly reduced over oceanic areas. This response is called inverted barometer behavior (we abbreviate it IB) [e.g., *Munk and MacDonald*, 1960; *Gill*, 1982]. On the other hand, we can also treat the ocean in the same way as the land, which leads to a larger variance than IB response; this is called the non-inverted barometer response (nonIB). Below, the pressure term is based on the inverted-barometer assumption, which would be appropriate shown in a recent study [e.g., *Dickman*, 1988; *Trupin and Wahr*, 1990; *Ponte*, 1994].

In the previous literature, the annual wobble excitation has been studied by decomposing the χ_i series into prograde and retrograde component [e.g., *Wilson and Haubrich*, 1976; *Wahr*, 1983; *Chao and Au*, 1991; *King and Agnew*, 1991]. This procedure was classically indispensable for the reason described below. Since the prograde component is amplified because of its proximity to the Chandler eigen frequency and has high signal to noise ratio, it would be accurately observed and have better quality than retrograde component. Indeed, *King and Agnew* [1991] indicated that the retrograde annual excitation estimated from the ILS data has systematically larger amplitude and a phase discrepancy of about 30 degrees, compared with those estimated from space–geodetically observed data. However, as clearly indicated in Fig. 2 of *King and Agnew* [1991], the retrograde annual excitations estimated from three different space–geodetic data are consistent with each other. Thus, we claim that the classical procedure is not necessary as long as one employs the space-geodetically obtained Earth orientation data.

3.5 Results

3.5.1 Intercomparison between NCEP AAM and JMA AAM

At the outset, we compare the NCEP AAM with Japan Meteorological Agency (JMA) AAM in order to check their mutual consistency, which will help examining the data quality (Figure 3.1). In light of Figs 3.1, both NCEP and JMA AAM are in good agreement for both pressure and wind term. Hence, as far as the seasonal variation is concerned, we can assess atmospheric contribution to the annual wobble either by NCEP or by JMA. In the present study, we would employ NCEP AAM computed by ourselves.

3.5.2 Comparison between Inferred and AAM excitation

In order to confirm the AAM contribution to the annual wobble excitation, we compared the mean inferred excitation with corresponding AAM in Figure 3.2: the AAM is further decomposed into pressure and wind term (Figure 3.3). Though the coordinate system can be arbitrarily selected, we followed the conventional system, i.e., X axis for Greenwich meridian and Y axis for 90 degrees west longitude. The (Coriolis) torque around the X axis corresponds to the χ_2, and that around the Y axis is χ_1: though the χ_i function has been frequently quoted as angular momentum (and we will also do below), they are, rigorously speaking, the torque.

We can summarize the AAM contribution to the seasonal wobble (see also, Table 3.1). Although the AAM is known to be an imperfect contributor to the annual wobble [e.g., *Wilson and Haubrich*, 1976; *Wahr*, 1983; *King and Agnew*, 1991; *Chao and Au*, 1991 among others], the present simple method, i.e., to view the excitation from X and Y axes, tells that the χ_2 AAM is in very good agreement with the observed excitation, and that most of the χ_2 AAM originates in the pressure term in light of Figure 3.3. Taking account of the year-to-year fluctuation of χ_2 AAM as well as inferred χ_2 excitation shown in Figure 3.4, we

variance	inferred	AAM(W+P)
$(10^{-14} rad^2)$		
χ_1	**0.16**	0.03
χ_2	**0.74**	0.87

Table 3.1: Variance of mean seasonal excitation, inferred and AAM. P and W denote pressure(inverted barometer) and wind term, respectively.

conclude that the annual signal for the inferred annual χ_2 variation is the atmospheric pressure term. Hence, the torque acting on the Earth's equatorial bulge, neither the mountain torque nor the frictional torque, is the cause for χ_2 annual signal. However, as indicated in Table. 3.1, the χ_1 AAM term is much smaller than that for inferred excitation, and this deficit turns out to have caused that the AAM alone cannot wholly explain the annual wobble excitation: we may roughly say that χ_1 AAM does not contribute to the annual wobble excitation.

3.5.3 Regional Contribution

In order to capture regional atmospheric contribution to the total AAM as well as to the inferred annual excitation, we computed the regional AAM at 36 times 36 sectors of the globe aside from the global AAM,

$$\chi_i(t) = \sum_{j=1}^{36}\sum_{k=1}^{36} X_i^{j,k}(t). \qquad i = 1, 2 \tag{3.4}$$

Thus, it follows that the temporal variance of the global $\chi_i(t)$ series can be expressed as the sum of the temporal covariances between $\chi_i(t)$ and each $X_i^{j,k}(t)$ series [*Salstein and Rosen*, 1989];

$$var\,\chi_i = \sum_{j=1}^{36}\sum_{k=1}^{36} cov(X_i^{j,k}, X_i^{j,k}). \tag{3.5}$$

The variance map would tell us the intensive area for seasonal fluctuation. Preceding the analysis, we compute the mean seasonal excitation for both global- and gridded-AAM, by stacking monthly values at each year into the same 12 months.

The temporal variation in the most vigorous area shown above, however, may not be in phase with the globally–integrated AAM fluctuation. In order to see whether the regional contribution is in–phase or out-of-phase with the global AAM, we would further compute the covariance field, i.e.,

$$cov\chi_i = \sum_{j=1}^{36}\sum_{k=1}^{36} cov(\chi_i, X_i^{j,k}). \tag{3.6}$$

Furthermore, by replacing the χ_i with the inferred excitation in the equation above, we can investigate where the Earth's wobble is excited by atmosphere if the global AAM shows close agreement with the inferred excitation.

Shown in Figure 3.5 are the variance for seasonal pressure term of each sector, given by var(χ_1)+var(χ_2): most of the variance originates in the χ_2 component as can be seen from Figure 3.2. Also shown in Figure 3.6 is the covariance map of the pressure term, given by cov(χ_1)+cov(χ_2). Clearly illustrated is the area which influences the χ_2 seasonal excitation, i.e., the central area of Eurasian continent.

Although these area are basically coincident with those suggested as effective region for annual wobble excitation by the former studies [e.g., *Jeffreys*, 1915; *Sidorenkov*, 1973], we can see that there are three regions of strong surface pressure variation if examined in detail: that is, the northern–east China, the Pakistan and the area around the Aral Sea. Furthermore, it should be noted that the pressure variation in the whole Eurasian area does not vary in phase everywhere. In view of Figure 3.6, the surface pressure variation around the Takramakan desert and Tibetan Plateau rather varies out-of-phase with the total χ_2 pressure variation: there is a localized center of cancellation area. Since the χ_2 inferred excitation can be mostly attributed to the AAM contribution in view of Figure 3.2, Figure 3.6 can be regarded as the contribution map for annual χ_2 component.

The variability of the pressure term depicted in Figure 3.5 is directly related to the

covariance field of Figure 3.6. However, it is not obvious to what extent the regional fluctuation in $X_i^{j,k}$ might cancel each other when their effects are globally integrated into χ_i. The variance and covariance map of wind AAM term illustrates that, unlike the case of pressure term, the region with intensive variability does not necessarily correspond to a significant area for the globally integrated χ_i term. Shown in Figure 3.7 is the wind variance map, given by var(χ_1)+var(χ_2). We see that the most extensively variable area resides around western Pacific region. It is to be noted that, unlike the axial angular momentum balance, the zonal wind around the equator does not contribute to the equatorial angular momentum balance as long as their longitudinal variation is small.

Meanwhile, Figure 3.8 indicated the regional contribution to the globally integrated χ_i wind term, given by cov(χ_1)+cov(χ_2). We can see that the regional wind variation over the Pacific hemisphere is roughly in phase with global χ_i wind term, while in the other hemisphere they are out of phase.

3.6 Discussion and Conclusion

Since the conventionally employed coordinate axes fortunately orient toward the Greenwich meridian and 90deg west longitude, we could clarify that the χ_2 component is largely explained by AAM. Though it is widely known that AAM cannot fully explain the annual wobble excitation, it has never been documented, to my knowledge, that the discrepancy originates mainly in the χ_1 component (Figure 3.2). The present understanding is provided by the simple approach to directly compare the χ_1 and χ_2 component with their corresponding excitations; this approach can fully utilize the quality of space-geodetic data.

To be concerned with the χ_2 component, the pressure term turns out to be most important as has been suggested by previous studies, and thus the mechanism is the torque acting over the Earth's equatorial bulge. Without employing globally distributed atmospheric pressure data, these insights could be obtained, to some extent, by looking into the

inferred excitation alone: the inferred excitation, when plotted in two dimensional plane, is significantly polarized toward Y-axis [see Fig. 9.1 in *Munk and MacDonald*, 1960]. Moreover, (though it is an incorrect understanding that [corrected by *Barnes et al.* 1983; *Wahr*, 1983]) the geostrophic wind and current have been shown not to excite the Earth's wobble. Thus, the former researchers could have placed particular emphasis on the pressure variation over Eurasian continent.

By employing uniformly distributed global atmospheric data, we examined the regional contribution, and confirmed the above classical idea. However, we believe that the results inferred in the present study are novel in the following respects. First, we clarified that there are three particularly important regions, where the surface pressure fluctuation contributes in–phase to the total χ_2 pressure variation. Secondly, nevertheless, there is one very localized cancellation center around the Tibetan Plateau among the three intensive regions above (Figure 3.5). In other words, the existence of this localized cancellation area suppresses the overshoot of other three intensive regions for the χ_2 pressure term. The wind term in χ_2 component plays a minor role, though it has a non–negligible contribution [*Chao and Au*, 1991].

As discussed above, the χ_1 AAM has failed to explain the corresponding observed excitation. However, by shedding light on the torque around Y-axis, we can speculate the possible source(s) which might explain the remaining discrepancy. For mass redistribution effect, the most efficient region which has a potential influence on the χ_1 term will reside around two longitudes, i.e., Greenwich meridian and 180deg east(west) longitude, since they have the longest arm length. The major possible contribution to the seasonal wobble other than atmospheric contribution would be presumably the land water effect(precipitation – evapotranspiration – run off) and ocean contribution among others (see *Chao* [1994] for possible contributors). Since the land water contribution cannot originate in the oceanic area, it would originate in the Greenwich meridian. However, we cannot expect an extensive seasonal fluctuation in rain and snow amount as prevailing over the Asian monsoon region or

over the northern America [*Chao and O'Connor*, 1988]. The remaining candidate for χ_1 would be the oceanic effect, which may contribute to the fluctuation of relative angular momentum via the seasonal variation of ocean current [*Furuya*, 1996 (this issue)].

Moreover, it is to be noted that the wind term in the χ_1 AAM is in phase with the observed χ_1, though the total χ_1 AAM results in out of phase due to the pressure term (Figure 3.3). We see that the wind term's in-phase behavior mostly originates over the Pacific Ocean in light of Figure 3.8. We think that this suggests a potential importance veiled in the Pacific ocean. From the equivalence of angular momentum approach and torque approach, the wind(motion) term is the sum of frictional torque plus mountain torque [e.g., *Munk and MacDonald*, 1960; *Lambeck*, 1980; *Barnes et al.* 1983; *Wahr*, 1982], so does the variation in the wind term over the oceanic area. Former studies indicate that for the atmosphere the frictional torque is the same order of magnitude as the mountain torque [e.g., *Newton*, 1971; *Wahr and Oort*, 1984]. Thus, some part of the frictional torque would originate in the ocean area, and its reaction would drive the oceanic general circulation. The sea surface wind stress will cause the seasonal variation in the oceanic mass transport, and thus can induce the oceanic excitation; note that we did not consider the oceanic response to the overlying atmospheric wind, since we allowed the atmospheric influence by angular momentum approach.

In practice, however, the sea surface frictional torque (wind stress torque) is not the only cause for oceanic momentum transport, and its effect has been estimated to be very small by *Wahr* [1983]. We must also take into account of bottom pressure torque as well as internal frictional torque in the ocean. In the literature of physical oceanography, it still remains unsolved questions how topography affects the ocean flow above, since it is almost impossible to directly measure bottom pressure and thus to confirm the idea [e.g., *Munk and Palmen*, 1951; *Holland*, 1973; *Hughes and Killworth*, 1995]. In a companion paper, we investigate the Pacific influence upon the annual wobble excitation, and will examine the physical processes to maintain the fluctuation of oceanic angular momentum.

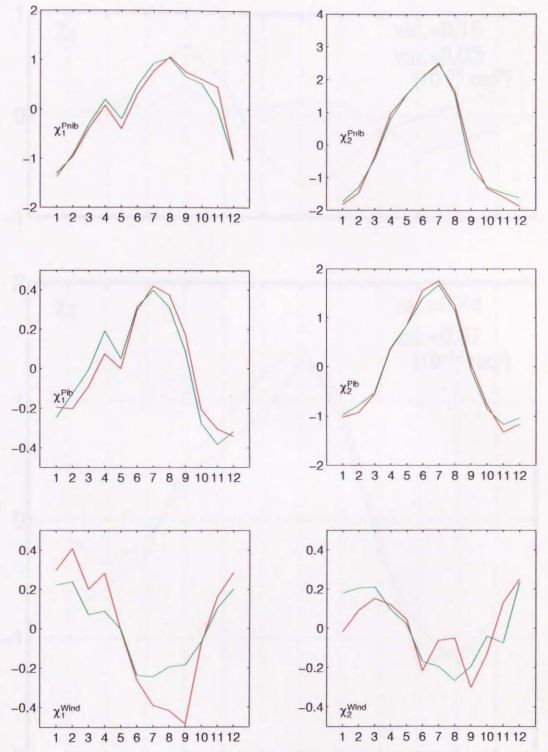

Figure 3.1: Red for JMA, Green for NCEP. Vertical Unit is 10^{-7} rad.

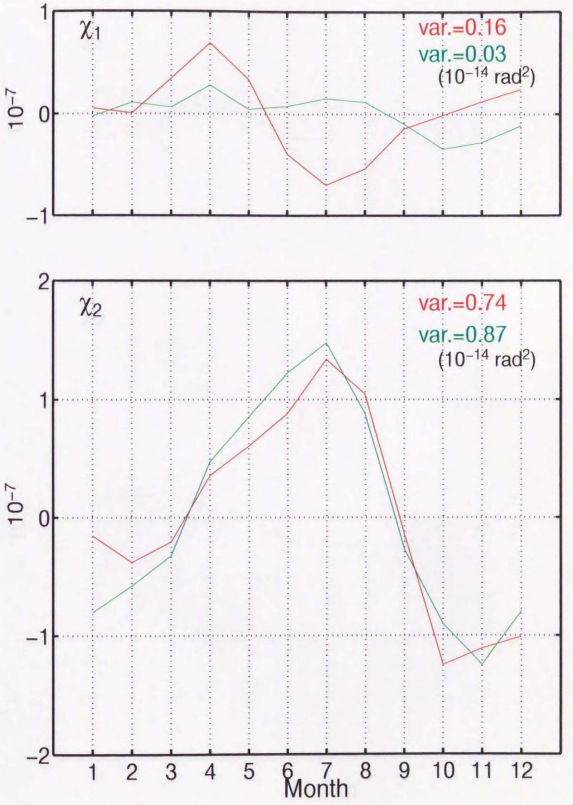

Figure 3.2: Mean yearly excitations for inferred (red) and pressure plus wind AAM (green). The variance of each component is indicated.

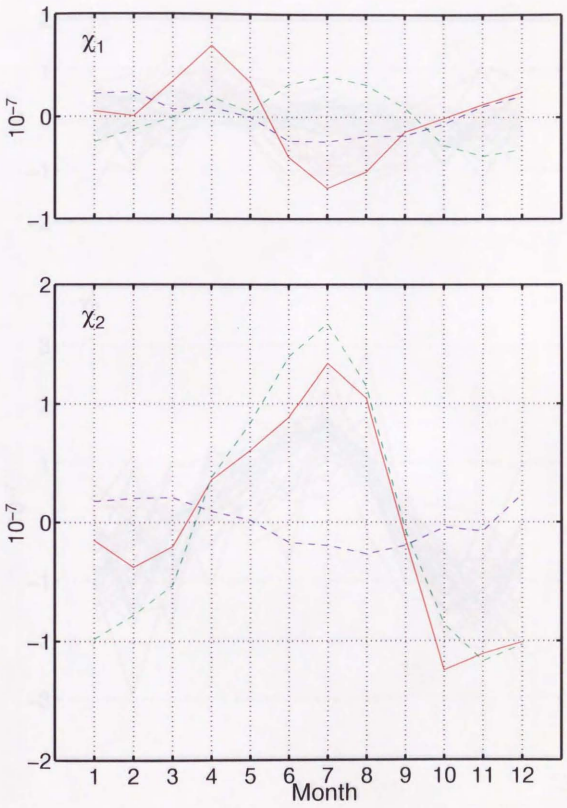

Figure 3.3: Mean yearly excitations for inferred (red), pressure(dashed green) and wind (dashed blue) AAM.

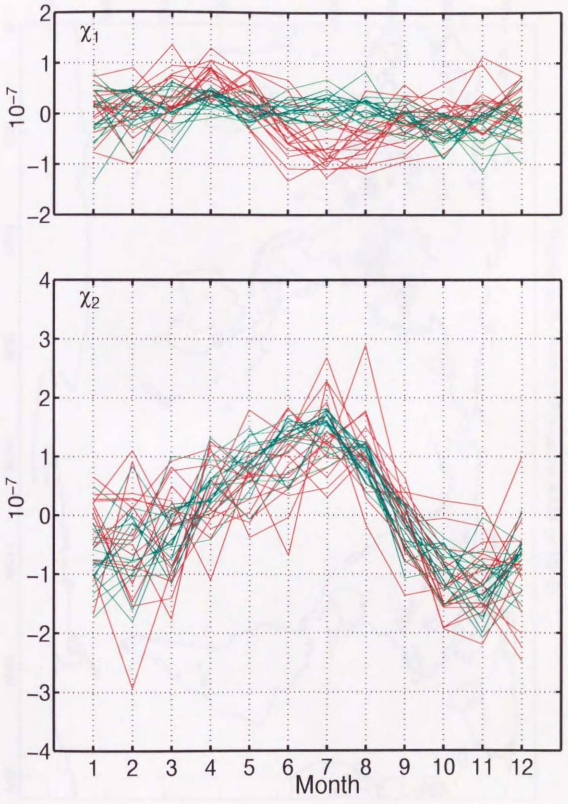

Figure 3.4: Yearly excitations of 16 years for inferred (red) and pressure plus wind AAM (green). We can see the amount of year to year fluctuation.

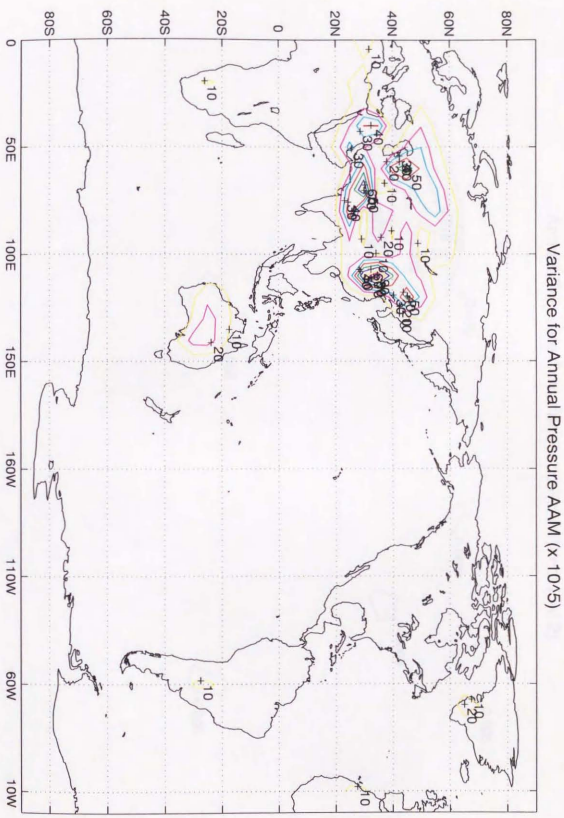

Figure 3.5: The variance of pressure term in each of the sectors of the vector function, X, seasonal component, 1979–1995, given by $\mathrm{var}(X_1^p)+\mathrm{var}(X_2^p)$.

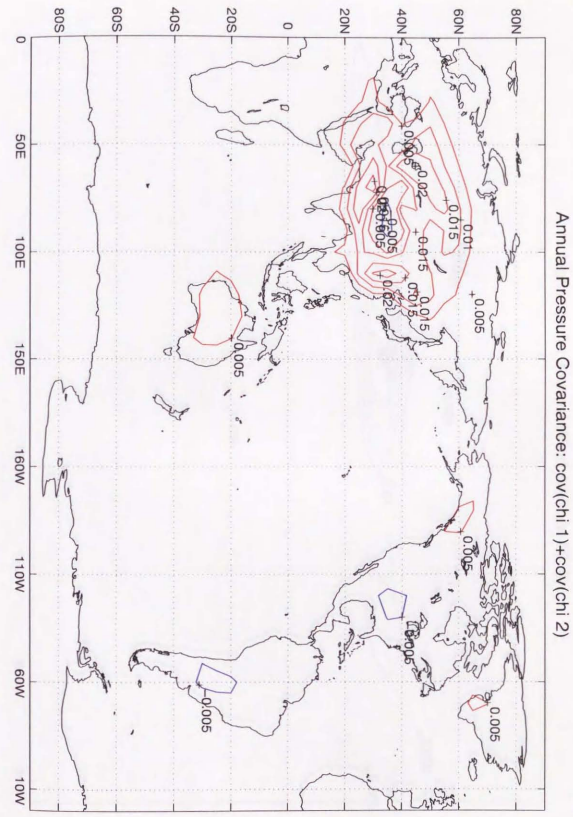

Figure 3.6: The covariance between the seasonal component of global X^P and the seasonal component of each sector value, given by $\mathrm{cov}(\chi_1^P,\ X_1^P)+\mathrm{cov}(\chi_2^P,\ X_2^P)$. Units are non-dimensional in 10^{-14}.

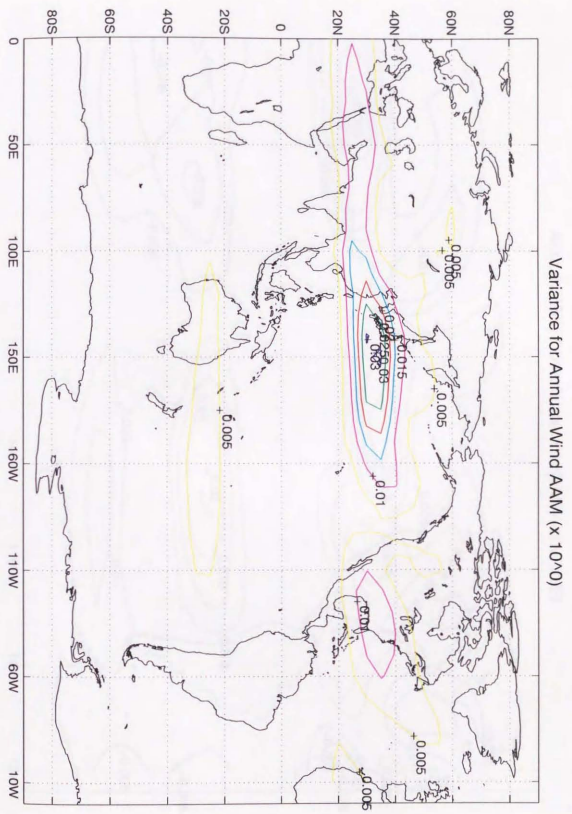

Figure 3.7: The variance of wind term in each of the sectors of the vector function, X, seasonal component, 1979–1995, given by $\mathrm{var}(X_1^W)+\mathrm{var}(X_2^W)$.

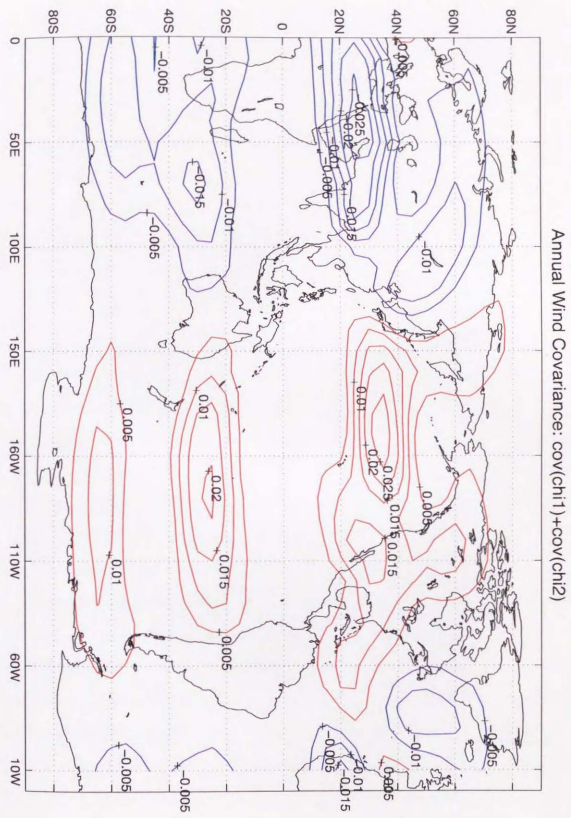

Figure 3.8: The covariance between the seasonal component of global X^W and the seasonal component of each sector value, given by $\mathrm{cov}(\chi_1^W, X_1^W)+\mathrm{cov}(\chi_2^W, X_2^W)$. Units are non–dimensional in 10^{-14}.

Chapter 4

Pacific Ocean Influence

4.1 Abstract

Pacific Ocean monthly analysis data from National Center for Environmental Prediction(NCEP) are employed to compute the Pacific Ocean angular momentum(POAM) for the period from 1980–1994. We assess its influence on the Earth's seasonal wobble excitation, paying particular attention to the torque, χ_1, which orients toward 90 deg. W longitude; the atmospheric angular momentum(AAM) hardly contributes to this torque. On the contrary to AAM, the POAM causes larger variance in χ_1 component than in χ_2, the torque orienting toward Greenwich meridian. The variance of the AAM plus POAM χ_1 is almost 10 times that of the AAM alone, while that of AAM plus POAM χ_2 is decreased to about 60 % of that of AAM alone. Taking account of year-to-year fluctuation, the observed seasonal excitation inferred from wobble data can be well-explained by AAM plus POAM for both its amplitude and phase. It is also found that the seasonal χ_1 POAM mostly consists of the current term, and that the mass term plays a secondary role; this is in contrast with the AAM contribution to the χ_2. The area with a remarkable seasonal fluctuation in the χ_1 current term is localized around the western Pacific region, especially around the east Philippine as well as the off-northern-east of Japan. We also employ the

torque approach to examine the mechanism in maintaining the seasonal fluctuation. The sea surface wind stress determines the seasonal rhythm of χ_1 current term, but accounts for less than half the total amplitude and does not show any significant inter-annual variation. The internal friction and bottom pressure torque are required to account for the total χ_1 current; the former has a significant seasonal variability, while the latter shows a short-period variation superimposed on inter-annual variation.

4.2 Introduction

The Earth's angular velocity vector varies its orientation as well as its amplitude over a wide range of time scales. Its orientation change relative to the terrestrial reference frame is known as polar motion (or wobble), of which two components, 14 months' Chandler wobble(CW) and 12 months' annual wobble(AW), are the main constituents, setting aside the slower polar drift. To identify the causes of Earth's wobble will be a constraint on the Earth's response property well-below the seismic band, and also help understanding the angular momentum exchange within the Earth's multi-sphere, i.e., atmosphere, hydrosphere, lithosphere(the mantle) and core.

The studies of atmospheric influence on the Earth's variable orientation have exploded over the past decade, presumably owing to the advent of global atmospheric data produced by routine objective analysis system (4–dimensional data assimilation system) as well as to the quality improvement of Earth rotation data. *Barnes et al.* [1983] carried out a pioneering work by applying the results of First GARP Global Experiment (FGGE, where GARP is the Global Atmospheric Research Program) to the Earth rotation data, and succinctly illustrated its impact on Earth rotation study. Their formulation for the atmospheric angular momentum(AAM) is presently a standard for Earth rotation study, and the AAM routinely computed in several agencies is rapidly transmitted via Global Telecommunications System to the Sub-bureau for AAM of International Earth Rotation

Service [*Salstein et al.* 1993]. Recently, several institutions have started to reanalyze(hindcast) the global atmospheric field, based on a homogeneous data assimilation system [*Kalnay et al.* 1996].

Employing the U. S. National Center for Environmental Prediction(NCEP) monthly reanalysis data, we revisited the atmospheric influence on the Earth's annual wobble to examine the regional contribution [*Furuya*, 1996 (this issue)]. Although it is well-known that, for annual wobble, there is a significant discrepancy between atmospheric effect and the corresponding inferred excitation [e.g., *Munk and MacDonald*, 1960; *Wilson and Haubrich*, 1976; *Lambeck*, 1980; *Chao and Au*, 1991; *Eubanks*, 1993], we showed that the discrepancy mainly originates in the χ_1 term, which represents a torque around axis toward 90degE longitude; the variance of χ_1 is less than 20 % of that inferred from wobble data. Meanwhile, the χ_2 is well-explained mainly by the pressure term. Hence, the remaining discrepancy should be explained by such sources that greatly affect the χ_1 with a small influence on the χ_2. Though we can think of many possible sources as seasonal wobble excitation, both land water and ocean effect have ever been investigated other than the atmosphere [*King and Agnew*, 1991]. However, considering that most of the disagreement between the AAM and seasonal wobble excitation originates in χ_1, we speculated that the angular momentum variation in the ocean will potentially explain much of the discrepancy, since we thought that the land water contribution as mass redistribution effect will not extensively contribute to χ_1 term; we note that the area affecting the χ_1 mass term resides around western Europe and Africa, where there is no distinct seasonality as prevailing over the Indian/Asian monsoon area.

There are, to my knowledge, only a few papers, in which oceanic influence upon the Earth's annual wobble is examined [*Munk and Groves*, 1952; *Wilson and Haubrich*, 1976; *O'Connor*, 1980; *Wahr*, 1983]; obviously, the lack of realistic global ocean data hampered reliable estimate of oceanic effect. *Munk and Groves* [1952] estimated the ocean current effect on annual wobble excitation, based on the vertically integrated mass transport stream

function; it had been analytically obtained in the Munk's theory on western boundary currents [*Munk*, 1950]. They states, "the circulation in the Pacific Ocean alone accounts for 10 per cent of the magnitude...". In those days, however, the observation for the seasonal transport variation is hardly available, on which their estimate rely. Thus, *Munk and MacDonald* [1960], and reiterated by *Wilson and Haubrich* [1976], stated that the effect of wind-stressed non-isostatic sea level change on the wobble excitation is the remaining question. *O'Connor* [1980], based on the linearized one–layer barotropic model with flat-bottom ocean, analytically estimated the effects of wind-driven perturbation in bottom pressure on the annual excitation. He did not consider the effects of wind-driven currents. *Wahr* [1983] also employed a simple linear ocean model, i.e., the so-called Sverdrup balance with realistic ocean–continent distribution. This model was driven by the sea-surface wind stress climate values [*Hellerman and Rosenstein*, 1983]. Wahr's estimate in based on the flat-bottom barotropic model with the uniform depth of 4000m: all frictional, inertial and advective terms are ignored. Results suggested that the wind-driven ocean has little effects on the annual excitation.

Wahr [1983] gave a caveat on his results, in that the influence of two omissions of both bottom topography and density stratification is not appreciated. As he stated, bottom topography can potentially contribute to a mountain-torque between the ocean and solid Earth [this idea was pioneered by *Munk and Palmen*, 1951]. However, he considered that the most prominent 'mountains' are the ocean–continent boundaries, and that the omission might not be too serious a problem. In other words, *Wahr* [1983] examined a torque acting at precipice of 4000 m high between the ocean and solid-Earth, and neglected the baroclinicity as well as the bottom topography. In the literature of physical oceanography, it has been unsolved questions how topography affects the ocean flow above, since it is almost impossible to directly measure bottom pressure and thus to confirm the idea [e.g., *Holland*, 1973; *Hughes and Killworth*, 1995].

Recently, the numerical modeling of ocean general circulation has grown explosively,

owing to the improvement of understanding the ocean dynamics and the advent of high performance computing facility [see, e.g., *McWilliams*, 1996]. The output data from the *Semtner and Chervin* [1992] (and its modification to the free surface model) model have been employed to assess the oceanic effect on the wobble excitation [e.g., *Steinberg et al.* 1995; *Salstein et al.* 1995] and length of day (lod) change [*Ponte and Rosen*, 1994]; *Bryan* [1995] (unpublished manuscript) also examined the oceanic influence on the length of day change, based on the Geophysical Fluid Dynamics Laboratory Modular Ocean Model. Still, it should be noted that these model output data are simply the result of 'simulation', and may not be compared with real-time Earth-orientation or lod data. Moreover, the largest defect in these output data is that the model is driven by atmospheric climate values, and not coupled with the atmosphere above: the atmosphere–ocean interaction is not taken into account.

The ocean data assimilation, as has been done for atmosphere, is presently an active research area in physical oceanography as evidenced by the growing literature, but still in the infancy due, largely, to the lack of observation. Nevertheless, the basin-scale analyses (the Pacific and Atlantic) are presently being done at NCEP [*Leetmaa and Ji*, 1989; *Ji et al.* 1994; *Ji et al.* 1995]: the analysis data set of the Pacific Ocean is presently archived at Climate Diagnostics Center, NOAA (Anonymous ftp at ftp.cdc.noaa.gov:Datasets/leetmaa).

The purpose of this paper is two folds; the first is to report the impact of the Pacific Ocean on the Earth's seasonal wobble excitation, employing the NCEP ocean analysis data, and the second is to examine the physical processes involved in maintaining the fluctuation of the Pacific ocean angular momentum (POAM). As stated in *Ji et al.* [1995], it depends largely on the availability of observational data to what extent the assimilated data is close to the reality; at present, only thermal information is used in their system (e.g., sea surface temperature and sparse subsurface thermal profiles), and the information about surface currents and sea level variation from altimeters is now getting available [*Ji et al.* 1996; *Hurlburt et al.* 1996]. There would be much room to improve the quality of ocean

analysis system, and the global ocean analysis system will surely be implemented in the near future. Since we take account of the Pacific Ocean alone, the present result should be regarded as preliminary. Nevertheless, the results shown below are encouraging for both our conjecture, i.e., the potential importance of the ocean for annual wobble excitation, and the effort to implement the ocean analysis system.

4.3 Pacific Influence on the Seasonal Wobble

4.3.1 Data and Formulae for Oceanic Angular Momentum

For the computation of oceanic angular momentum(OAM), we use the fields of temperature, salinity, eastward(u) and northward(v) velocity components of ocean current all at multiple depths (27 levels) of the monthly NCEP ocean analysis data. Moreover, the surface variables, i.e., east-west stress, north-south stress and surface pressure variation are employed in later section; note that this surface pressure variation data set is diagnostically computed from ocean thermal state in order to evaluate the sea level change, and does not represent the atmospheric pressure at sea surface (see the texts below). The undulated bottom topography is taken into account. The spatial coverage is, 1.0 deg latitude × 1.5 deg longitude boxes covering 45N-35S latitude, 122.25E-288.75E longitude (see Figure 4.1): these grids are for analysis purpose, and the latitudinal grid spacing in the original model is actually 1/3-degree within 10 deg of the equator and gradually increases outside this zone as in *Philander et al.* [1987]. We used the monthly data from Jan. 1980 to Dec. 1994; we downloaded the analysis data set of the Pacific Ocean from Climate Diagnostics Center, NOAA (Anonymous ftp at ftp.cdc.noaa.gov:Datasets/leetmaa). The details on the ocean model, the assimilation system, the data used for assimilation and the quality control system are described in *Ji et al.* [1995] (and the references therein).

The computation of OAM is almost the same as that of AAM [*Barnes et al.* 1983],

except the mass term corresponding to the pressure term of AAM; note that ocean bottom pressure data set is not readily available. If we prescribe the equilibrium state of ocean as being in hydrostatic balance with no motion, the first order perturbation in the mass term will consist of changes in both density structure and sea level changes. Thus, the mass term is composed of two terms as shown by *Ponte and Rosen* [1994]. For the motion term, we integrate the u and v along the vertical axis, ignoring the changes in both density field and sea level. Hence, the following formulae (4.1) are required in evaluating the OAM,

$$\begin{aligned}
\chi_1 &= -\frac{1.098R^4}{(C-A)g}\int\int P_{density}\sin\phi\cos^2\phi\cos\lambda d\lambda d\phi \\
&\quad -\frac{1.098R^4}{(C-A)g}\int\int \eta_{surface}\sin\phi\cos^2\phi\cos\lambda d\lambda d\phi \\
&\quad -\frac{1.591R^3}{\Omega(C-A)g}\int\int\int(u\sin\phi\cos\phi\cos\lambda - v\cos\phi\sin\lambda)dpd\lambda d\phi, \qquad (4.1\text{-a}) \\
\chi_2 &= -\frac{1.098R^4}{(C-A)g}\int\int P_{density}\sin\phi\cos^2\phi\sin\lambda d\lambda d\phi \\
&\quad -\frac{1.098R^4}{(C-A)g}\int\int \eta_{surface}\sin\phi\cos^2\phi\sin\lambda d\lambda d\phi \\
&\quad -\frac{1.591R^3}{\Omega(C-A)g}\int\int\int(u\sin\phi\cos\phi\sin\lambda + v\cos\phi\cos\lambda)dpd\lambda d\phi, \qquad (4.1\text{-b}) \\
\chi_3 &= \frac{0.753R^4}{C_m g}\int\int P_{density}\cos^3\phi d\lambda d\phi \\
&\quad +\frac{0.753R^4}{C_m g}\int\int \eta_{surface}\cos^3\phi d\lambda d\phi \\
&\quad +\frac{0.998R^3}{\Omega C_m g}\int\int\int u\cos^2\phi dp d\lambda d\phi. \qquad (4.1\text{-c})
\end{aligned}$$

The χ_1 and χ_2 represent the angular momentum around equatorial axes as noted before, while the χ_3 does that around polar axis. Here, R, g, and Ω are the Earth's mean radius, mean surface gravity, and mean angular velocity, respectively; C and A are the Earth's polar and equatorial moments of inertia, while C_m is the polar moments of inertia for the mantle alone; $P_{density}$ is the bottom pressure fluctuation caused by density change, and $\eta_{surface}$ is the sea level change which is evaluated from the procedure stated below. The ϕ and λ are latitude and longitude, respectively. The numerical factors multiplied in the r. h. s of eqs. (4.1) account for the Earth's loading and rotational deformation as a function

of Love numbers [e.g., *Munk and MacDonald*, 1960; *Wahr*, 1982; *Eubanks*, 1993].

The ocean model is basically the same as that of *Philander et al.* [1987], in which the sea surface is treated as rigid lid. Thus the sea level variation is not a prognostic variable, and the sea level term in eqs. (4.1) shown in this paper may be regarded as preliminary estimates as in *Ponte and Rosen* [1994]. However, even if the surface is treated as rigid lid, it is to be noted that the lateral pressure variation exists at the surface. *Ji et al.* [1995] illustrated that the model-produced surface dynamic height anomaly relative to 1000 db, which is very closely related to surface pressure, captured most of the low frequency variability in the sea level data that was independently observed by tide-gauge. Thus, the archived surface pressure data, when divided by gravity, would be good proxy for sea level variation. We evaluate the bottom pressure at each site by computing the three dimensional density fields with the equation of state for sea water [*Gill*, 1982] and integrating it vertically.

4.3.2 Results

In the previous literature on the seasonal wobble, the excitation inferred from wobble data was decomposed into prograde and retrograde component for the reason discussed below [e.g., *Munk and MacDonald*, 1960; *Wilson and Haubrich*, 1976; *Wahr*, 1983; *Chao and Au*, 1991; *King and Agnew*, 1991]. The prograde component is more amplified because of its proximity to the Chandler eigenfrequency and has higher signal to noise ratio than the retrograde one; the signal of the latter is almost immersed in the noise level [see the footnote in page. 94 of *Munk and MacDonald*, 1960; see also Table. 1]. However, as long as we use the space-geodetically observed Earth orientation data, the retrograde component is also beyond the noise level (Table. 1). Indeed, the Fig. 2 in *King and Agnew* [1991] clearly indicated that the retrograde annual excitations estimated from three different space-geodetic data are consistent with eath other. Hence, we do not have to use the conventional technique, and will directly compare the observed $\chi_i (i = 1, 2)$ with the

corresponding components.

Preceding to see the influence of POAM, we revisit the effect of AAM on the seasonal wobble excitation. Figure 4.2 shows the mean seasonal observed (red) and NCEP AAM (green) excitation series from 1980 to 1994. Each monthly value of the mean seasonal series is obtained by averaging the values at each month for the 15 years' period, after removing the long-term trend and offset with three degree polynomial. As discussed in *Furuya* [1996], the AAM explains most of the χ_2 term, while it does not the χ_1 term; the AAM hardly contributes to the χ_1. Here, the observed excitation, $\tilde{\psi}$, is inferred by inserting the daily wobble data, SPACE95 [see, *Gross*, 1996], into the following $\tilde{\mathbf{m}}$,

$$\frac{i}{\sigma_{cw}} \frac{d\tilde{\mathbf{m}}}{dt} + \tilde{\mathbf{m}} = \tilde{\psi}, \tag{4.2}$$

where the σ_{cw} is complex Chandler eigenfrequency. For this deconvolution, we used the filter (2a) in *Wilson* [1985]; the Chandler period and Q-value are prescribed to be 434 days and 100, respectively [e.g., *Wilson and Vicente*, 1990; *Furuya and Chao*, 1996]. Afterwords, we compute its monthly averaged series in order to comform to both the OAM and AAM series. The correspondence between $\tilde{\chi}$ and $\tilde{\psi}$ is the following,

$$\tilde{\psi} = \tilde{\chi} - \frac{i}{\Omega} \frac{d}{dt} \tilde{\chi}. \tag{4.3}$$

Here, the values with over-tilde, $\tilde{X}$, is defined as $X_1 + iX_2$. Under long period approximation [*Gross*, 1992], the difference between $\tilde{\chi}$ and $\tilde{\psi}$ is negligible.

Shown in Figure 4.3 is the result of POAM plus AAM (blue). We can see a significant Pacific Ocean contribution to the χ_1, which was not well explained by AAM alone. Rather, the fluctuation in the POAM plus AAM is larger than observed χ_1 component; the excess contribution might be canceled out by other unaccounted sources (e.g., the contribution from the other oceanic basin, the land water etc). Figure 4.4 illustrates the POAM alone. The χ_1 term shows larger variability than the χ_2 term, which is in contrast with the case for AAM: for the present coordinate axes, the Pacific ocean area can efficiently contribute to

χ_1 rather than χ_2. Also, in 1983, 1987 and 1992, we note a pronounced amplitude in the χ_1 around February compared with those in other years, and that the three years correspond to El-Niño year. Thus, the larger fluctuation in these years is probably caused by some El-Niño effect, and merits further attention. However, it is interesting that we do not see corresponding signals in the inferred excitation (Figure 4.3). If the inferred excitation is correctly the wobble excitation, one can think of other unaccounted signal(s) suppressing the large amplitude. Otherwise, they may simply be an overestimate for POAM variation.

For reference, we compare in Figure 4.5 the axial component of AAM with the corresponding POAM. The Pacific contribution to axial angular momentum budget is very small, compared with the AAM [e.g., *Ponte and Rosen*, 1994].

We will examine the mean annual cycle in Figure 4.6; the mean annual cycle is obtained by averaging the values at each month for the whole years. For the inferred seasonal excitation, the variance of χ_1 is 0.16, while that of χ_2 is 0.74; the unit is 10^{-14} rad^2. As noted in *Furuya* [1996], the AAM contribution is much more polarized due to the small variance of the χ_1 term: the χ_1 variance for AAM is less than 20 % of that for the inferred excitation, while the χ_2 AAM is in good agreement with that of inferred excitation.

We would place particular attention to the χ_1 term for which the AAM could hardly account. The mean seasonal cycle of AAM plus POAM roughly captures that inferred from wobble. In particular, it reproduces both the minimum around July and the increasing amplitude toward winter season, although the exception resides in the AAM plus POAM χ_1 term around February. In light of Figure 4.7, we see that the agreement depicted in Figure 4.6 is a robust feature, since the year-to-year POAM plus AAM fluctuation are within those of the seasonal wobble excitation. Moreover, we note that the χ_2 component is not much affected by the Pacific Ocean contribution (see also, Figure 4.4); the variance of χ_2 is reduced to about 60 % of the variance for AAM alone. Thus, we conclude that the Pacific contribution is far from negligible, and that it can explain the overall feature, i.e., both amplitude and phase of observed χ_1 component which the χ_1 AAM failed to explain.

Next, we will analyze the relative importance of three terms in eq. (4.1). In particular, we confine our attention to the χ_1 term of eq. (4.1-a), since it is shown to be more important for the seasonal wobble excitation. The upper panel in Figure 4.8 indicates the motion versus mass term: the total χ_1 POAM is shown with red dotted line. The mass term is decomposed into the sea level and density term in the lower panel of Figure 4.8. The top of Figure 4.8 clearly illustrates that most of the seasonal POAM originates in the motion term, and that the seasonal fluctuation in the mass term is small (see, eq. (4.1)). We can observe, for both motion and mass term, an inter-annual variation with time scales of roughly three to four years. In view of the separate contribution from sea level and density term shown in the bottom of Figure 4.8, a clear out-of-phase pattern can be recognized, which could be simply understood as a consequence of mass conservation; the warmer the water column, the higher the column height, and vice versa.

The motion term is caused by both frictional and mountain torque, while the matter term is a consequence of pressure variation acting on the Earth's equatorial bulge as discussed in later section. Thus, it turns out that, for Pacific Ocean seasonal wobble excitation, the torque acting on the Earth's ellipticity is small compared with those originating in the bottom topography, wind stress and friction (see below). This result is in contrast with the AAM annual wobble excitation. The AAM wind term plays a secondary role, whereas the POAM current term is primarily important.

4.4 Regional Contribution of Pacific Angular Momentum

We investigate the regional contribution of POAM, in order to shed light on the important area for the Pacific Ocean contribution. We will confine our attention to the χ_1 motion(current) term, which comprises most of the POAM as shown in previous section.

We computed mean seasonal cycle at each 1.0 deg ×1.5 deg grid for 15 years' period. Figure 4.9 (Top) is a contour map of the seasonal variance at each grid (see below); its cross section at each latitude is also shown in Figure 4.9 (bottom). It clearly indicates that the seasonal variation is very localized in the north-western Pacific region. In particular, we can pick up two areas, i.e., the right east of Philippine and the off-northern east coast of Japan, where one finds large seasonal variation.

Figure 4.9, however, does not tell how the regional variation contributes to the total POAM variation. To see what extent the regional variations in Figure 4.9 will cancel each other when they are combined to the whole POAM, we followed the method employed in *Salstein and Rosen* [1989] and computed covariance matrix at each grid, using both the mean regional, $X_i^{j,k}$, and basin-wide seasonal variation, $\chi_i^{j,k}$,

$$cov\chi_i = \sum_{j=1}^{all}\sum_{k=1}^{all} cov(\chi_i, X_i^{j,k}). \tag{4.4}$$

Plotted in Figure 4.10 is the off-diagonal element of r.h.s. of the equation above for the mean seasonal χ_1 motion term; note that Figure 4.9 is the map for the diagonal element of the above. The two areas around the Philippine and off-northern east Japan are acting in-phase and out-of phase, respectively with total Pacific χ_1 motion term.

Figure 4.11 illustrates a seasonal march of the regional χ_1 motion values for four seasons averaged over three months; we do not plot values less than some subjectively prescribed value. Figure 4.11 tells that a pronounced variation is achieved from autumn to the next spring, and that in summer the amplitude is small. The small amplitude presumably corresponds to the minimum around July in Figure 4.6; note that in Figure 4.6 the offset(mean value) is removed. In Figure 4.11, the steady component is removed and shown in Figure 4.12. Figure 4.12 indicates a strong positive signal due to Kuroshio over north-western Pacific region, while near the coastal boundaries the contribution is in negative sense.

4.5 Excitation Mechanism: Torque Approach

4.5.1 Formulation

In the literature of Earth's variable rotation study, to compare the angular momentum with inferred excitation is called angular momentum approach, while to compare the total (atmospheric or oceanic) torque with observed excitation is known as torque approach as described below [e.g., *Munk and MacDonald*, 1960; *Wahr*, 1982; *Barnes et al.* 1983; *Wahr and Oort*, 1984]. As long as the wind data set at multiple levels is available, the angular momentum approach is preferred. However, the spatially integrated angular momentum itself does not tell what forces are responsible for the Earth's wobble excitation. By examining the relative importance of each term in the torque approach (see below), we can understand what physical processes are important for the Earth's wobble excitation; though such an analysis has been done for atmospheric forcing of length of day change [e.g., *Wahr and Oort*, 1984; *Salstein and Rosen*, 1994], we do not know any previous work which focuses on the mechanism(s) for oceanic excitation of Earth's wobble.

The wobble excitation function ψ in eq. (4.2) is given by the following [e.g., *Munk and MacDonald*, 1960; *Barnes et al.* 1983]:

$$\Omega^2(C-A)\psi_1 = -\int_V \rho r(B_\lambda \sin\phi \sin\lambda + B_\phi \cos\lambda)dV, \tag{4.5-a}$$

$$\Omega^2(C-A)\psi_2 = -\int_V \rho r(B_\phi \sin\lambda - B_\lambda \sin\phi \cos\lambda)dV, \tag{4.5-b}$$

where, for angular momentum approach,

$$B_\lambda = d\,u/d\,t - 2\Omega v \sin\phi + 2\Omega w \cos\phi - (uv/r)\tan\phi + uw/r, \tag{4.6-a}$$

$$B_\phi = d\,v/d\,t + 2\Omega u \sin\phi + \Omega^2 r \sin\phi\cos\phi + (u^2/r)\tan\phi + vw/r, \tag{4.6-b}$$

and, for torque approach,

$$B_\lambda = -\frac{1}{\rho r\cos\phi}\frac{\partial P}{\partial\lambda} + F^{(\lambda)}, \tag{4.7-a}$$

$$B_\phi = -\frac{1}{\rho r}\frac{\partial P}{\partial\phi} + F^{(\phi)}. \tag{4.7-b}$$

Note that eqs. (4.6) are the longitudinal and latitudinal components of the Navier-Stokes equation for the atmosphere or ocean, and that eqs. (4.7) are the corresponding forcing terms representing, in order, the pressure gradient and frictional stress, respectively; the centrifugal potential term is included as the third term in the r.h.s. of eq. (4.6-b).

We have employed the angular momentum function, $\tilde{\chi}$, which consists of both matter and motion term [*Barnes et al.* 1983]. Since the motion term is shown to dominate over the matter term for the χ_1 POAM, we will focus our attention to the torques causing the motion term, and represent the $\tilde{\chi}$ motion term in terms of the corresponding $\tilde{\psi}$ function, based on eqs. (4.7).

In analogy with the case of AAM, the motion term in eqs. (4.1) is composed of both frictional torque and mountain(seafloor topography) torque, whereas the mass term derived from centrifugal potential in eqs. (4.1) corresponds to the 'mountain' torque acting on the Earth's equatorial bulge [e.g., *Wilson and Haubrich*, 1976; *Wahr*, 1982; *Wahr*, 1983; *Barnes et al.* 1983]. If we further decompose the whole frictional stress into the wind stress, $\tau^{\lambda}, \tau^{\phi}$(see below), applied at the sea surface and other frictional terms of eqs. (4.9), the motion term consists of the following three torques:

$$\tilde{\chi}_{Motion} = \tilde{\psi}_{Wind} + \tilde{\psi}_{Mountain} + \tilde{\psi}_{Friction}. \tag{4.8}$$

Note that the wind stress torque accounts for the interaction between atmosphere and ocean, while the mountain(seafloor topography) torque and friction torque represent the interaction between ocean and the solid Earth at sea bottom. Here, the archived wind stress data are converted from the surface wind fields of NCEP global atmospheric analysis, using a drag coefficient of 1.3×10^{-3} [*Ji et al.* 1995]. The frictional terms are as follows:

$$\begin{aligned} F^{(\lambda)} &= A_H\{\frac{1}{R^2\cos^2\phi}\frac{\partial^2 u}{\partial\lambda^2} + \frac{1}{R^2\cos^2\phi}\frac{\partial}{\partial\phi}(\cos\phi\frac{\partial u}{\partial\phi}) \\ &\quad -\frac{1}{R^2\cos^2\phi}(u + 2\frac{\partial}{\partial\lambda}v\sin\phi)\} + A_V\{\frac{1}{R^2}\frac{\partial}{\partial r}(r^2\frac{\partial u}{\partial r})\}, \qquad (4.9\text{-a}) \\ F^{(\phi)} &= A_H\{\frac{1}{R^2\cos^2\phi}\frac{\partial^2 v}{\partial\lambda^2} + \frac{1}{R^2\cos^2\phi}\frac{\partial}{\partial\phi}(\cos\phi\frac{\partial v}{\partial\phi}) \end{aligned}$$

$$-\frac{v}{R^2\cos^2\phi} + \frac{2\sin\phi}{R^2\cos^2\phi}\frac{\partial u}{\partial\lambda}\} + A_V\{\frac{1}{R^2}\frac{\partial}{\partial r}(r^2\frac{\partial u}{\partial r})\}, \qquad (4.9\text{-b})$$

where A_V and A_H are vertical and horizontal eddy viscosity, respectively. The horizontal eddy viscosity, A_H, is set to $2\times10^7\mathrm{cm}^2\mathrm{s}^{-1}$ [*Ming Ji*, personal communication]. The vertical eddy viscosity, A_V, is presently assumed to be 10^{-4} times of the A_H [see, e.g., *Pedlosky*, 1987].

The wind stress torque applied on the sea surface are given as follows:

$$\psi_1^{Wind} = -\frac{1.5913R^3}{\Omega^2(C-A)}\int\int(\tau^{\lambda}\sin\phi\sin\lambda + \tau^{\phi}\cos\lambda)\cos\phi d\phi d\lambda, \qquad (4.10\text{-a})$$

$$\psi_2^{Wind} = -\frac{1.5913R^3}{\Omega^2(C-A)}\int\int(\tau^{\phi}\sin\lambda - \tau^{\lambda}\sin\phi\cos\lambda)\cos\phi d\phi d\lambda. \qquad (4.10\text{-b})$$

The $\tilde{\psi}_{Wind}$ can be derived, by prescribing the following vertical stress divergence in eqs. (4.7):

$$B_{\lambda} = -\frac{1}{\rho}\frac{\partial}{\partial z}\tau^{\lambda}, \qquad (4.11\text{-a})$$

$$B_{\phi} = -\frac{1}{\rho}\frac{\partial}{\partial z}\tau^{\phi}, \qquad (4.11\text{-b})$$

where τ^{λ} and τ^{ϕ} are the stresses applied at sea surface. Notice that this torque corresponds to the contribution from barotoropic flat-bottom ocean model [*Wahr*, 1982; 1983].

The mountain(seafloor topography) torque can be written down as follows;

$$\psi_1^{Mountain} = -\frac{1.5913R^2}{\Omega^2(C-A)}\int\int P_b(\frac{\partial H}{\partial\phi}\cos\phi\cos\lambda + \frac{\partial H}{\partial\lambda}\sin\phi\sin\lambda)d\phi d\lambda, \qquad (4.12\text{-a})$$

$$\psi_2^{Mountain} = -\frac{1.5913R^2}{\Omega^2(C-A)}\int\int P_b(\frac{\partial H}{\partial\phi}\cos\phi\sin\lambda - \frac{\partial H}{\partial\lambda}\sin\phi\cos\lambda)d\phi d\lambda, \qquad (4.12\text{-b})$$

where P_b amd H are bottom pressure and ocean depth, respectively [*Wahr*, 1982; see also, Appendix. 1].

To evaluate the mountain(seafloor topography) torque in eqs. (4.12), however, requires some attention. As discussed in *Barnes et al.* [1983], the pressure gradient term in eqs. (4.7) accounts for the torque acting on both the seafloor topography and equatorial bulge. In other words, the 'topography' caused by Earth's ellipticity is also included in eqs. (4.12),

and the actual 'sea floor topography' torque is the difference, eqs. (4.12) minus the mass term of eqs. (4.1), i.e., the sum of both density and sea level term (see, Figure 4.13 and 4.7). Although *Wahr* [1982] provides a quite similar equation as eqs. (4.12) for the mountain torque, our eqs. (4.12) contain the ellipticity torque as well as the mountain torqe since we follow the formulation of *Barnes et al.* [1983].

Since the friction terms, eqs. (4.9), do not allow any simplification as done for wind stress and mountain torque, we directly carry out the numerical integration of eqs. (4.5), though constant density is assumed for simplicity. The frictional torque, $\psi_1^{Friction}$ and $\psi_2^{Friction}$, acts at the interface between the ocean and solid Earth since the frictional terms in eqs. (4.9) are integrated over the whole depth except the uppermost level.

4.5.2 Results

We examine the relative importance of three torques, i.e., wind stress torque, friction torque and mountain(sea floor topography) torque, for the χ_1 motion term. At the outset, we check the consistency of budget analysis by Figure 4.14a, in which the χ_1 motion term(red) and the sum of three torques(blue) are shown. The agreement is satisfactory, and thus we could move on the following budget analysis.

Figure 4.14b illustrates the wind stress torque applied at sea surface. The amplitude is insufficient to account for the total variation, but the phase agreement is very good. Moreover, the seasonal cycle of the wind stress torque is very regular, and its inter-annual variation is not so pronounced compared with other terms discussed below. Furthermore, it is to be noted that the wind stress contribution coincides with the motion term which would be inferred from linear barotropic ocean model with constant depth. Thus, we can be convinced that *Wahr* [1983] underestimates the ocean current contribution.

Figure 4.14c and 4.14d represent contributions from frictional (eq. (4.9)) and mountain(sea floor topography) torque, respectively. Obviously, these two terms are indispensable to account for the total variability of the motion term. The amplitude of both the frictional and wind stress terms is roughly comparable to each other. Comparing the three torque, the seasonal cycle shown in Figure 4.14c and 4.14d is not as stable as that in the wind stress torque. Moreover, Figure 4.14c clearly shows an irregular seasonal variation rather than the regular pattern of Figure 4.14b, whereas the seasonal fluctuation in topography term of Figure 4.14d is not so pronounced. The mountain torque appears to cause shorter period change as well as inter-annual variation.

4.6 Concluding Remarks

We computed ocean angular momentum of the Pacific Ocean and examined its influence on the Earth's seasonal wobble, using the NCEP ocean analysis data for the period of 1980–1994. We put our particular emphasis on the χ_1 term, to which the atmosphere hardly contributes. The seasonal χ_1 variation turned out to be roughly explained by adding the effect of Pacific Ocean. In particular, its motion(current) term is very important for both amplitude and phase.

Examining the regional contribution for the seasonal motion term, the north-western Pacific turns out to show an intensive variability. In particular, we found that two areas in northwestern Pacific are very important, i.e., the east of Philippine and the northern-east Japan; the variation over the Philippine sea is in-phase with the total χ_1 motion term.

Moreover, in order to investigate the mechanisms responsible for the dominant χ_1 motion term, we carried out a budget analysis of three torques which contributes to the motion term. The amplitude by wind stress torque is less than half the total amplitude, although this torque is important to determine the annual rhythm of motion term; the phase of wind stress torque agrees fairly well with the motion term. In order to account for the remaining amplitude as well as the inter-annual variation, other torques, e.g., friction and mountain torque, are indispensable.

It will be a very important and exciting topic to firmly evaluate the oceanic excitation of Earth's wobble, including the contributions from other oceans such as the Atlantic and Indian ocean.

4.7 Appendix. 1

We will show below the derivation of eqs. (4.12). The pressure gradient term yields the following excitation for the ψ_1 component,

$$\Omega^2(C-A)\psi_1 = -R^2 \int\int\int_{-H}^{0} (\frac{\partial P}{\partial \lambda}\sin\phi\sin\lambda + \frac{\partial P}{\partial \phi}\cos\phi\cos\lambda) dz d\phi d\lambda. \tag{4.13}$$

Similar expression can be obtained for the ψ_2 component as well. From the *Leibnitz'* rule,

$$\frac{\partial}{\partial x}\int_{B(x,y)}^{A(x,y)} f(x,y,z)dz = \int_B^A \frac{\partial f}{\partial x}dz + f(x,y,A)\frac{\partial A}{\partial x} - f(x,y,B)\frac{\partial B}{\partial x}, \tag{4.14}$$

the vertical integral of the pressure gradient term would be,

$$\int_{-H}^{0} \frac{\partial P}{\partial \lambda}dz = P_B\frac{\partial H}{\partial \lambda} + \frac{\partial \Pi}{\partial \lambda}, \tag{4.15-a}$$

$$\int_{-H}^{0} \frac{\partial P}{\partial \phi}dz = P_B\frac{\partial H}{\partial \phi} + \frac{\partial \Pi}{\partial \phi}, \tag{4.15-b}$$

where

$$P_B = P(\phi,\lambda,-H),$$
$$\Pi = \int_{-H}^{0} P dz.$$

By inserting the second term of eqs. (4.15) into the eq. (4.13) and integrating globally, we can see that the contribution from the Π disappears:

$$\begin{aligned}\int\int(\frac{\partial \Pi}{\partial \lambda}\sin\phi\sin\lambda + \frac{\partial \Pi}{\partial \phi}\cos\phi\cos\lambda)d\phi d\lambda &= \int \sin\phi[\int \frac{\partial \Pi}{\partial \lambda}\sin\lambda d\lambda]d\phi \\ &\quad + \int \cos\lambda[\int \frac{\partial \Pi}{\partial \phi}\cos\phi d\phi]d\lambda \\ &= \int\int(-\Pi\sin\phi\cos\lambda + \Pi\sin\phi\cos\lambda)d\phi d\lambda, \\ &= 0.\end{aligned}$$

since

$$\begin{aligned}\int \frac{\partial \Pi}{\partial \lambda}\sin\lambda d\lambda &= [\Pi\sin\lambda]_0^{2\pi} - \int \Pi\cos\lambda d\lambda, \\ \int \frac{\partial \Pi}{\partial \phi}\cos\phi d\phi &= [\Pi\cos\phi]_0^{2\pi} + \int \Pi\sin\phi d\phi.\end{aligned}$$

Hence, only the bottom pressure torque in eqs. (4.15)is taken into account for the integral of eq. (4.13). Thus, we arrive at the following:

$$\Omega^2(C-A)\psi_1 = R^2\int\int P_B(\frac{\partial H}{\partial \lambda}\sin\phi\sin\lambda + \frac{\partial H}{\partial \phi}\cos\phi\cos\lambda)d\phi d\lambda. \tag{4.16}$$

Similarly,

$$\Omega^2(C-A)\psi_2 = R^2\int\int P_B(\frac{\partial H}{\partial \phi}\cos\phi\sin\lambda - \frac{\partial H}{\partial \lambda}\sin\phi\cos\lambda)d\phi d\lambda. \tag{4.17}$$

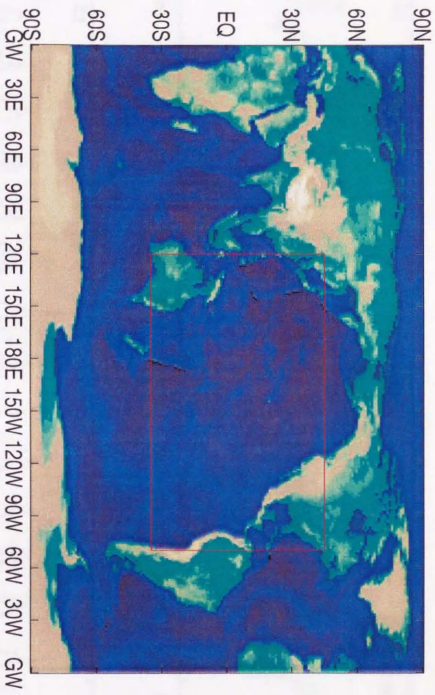

Figure 4.1: The Pacific Ocean bounded by red is the area accounted for the computation of Pacific Ocean Angular Momentum.

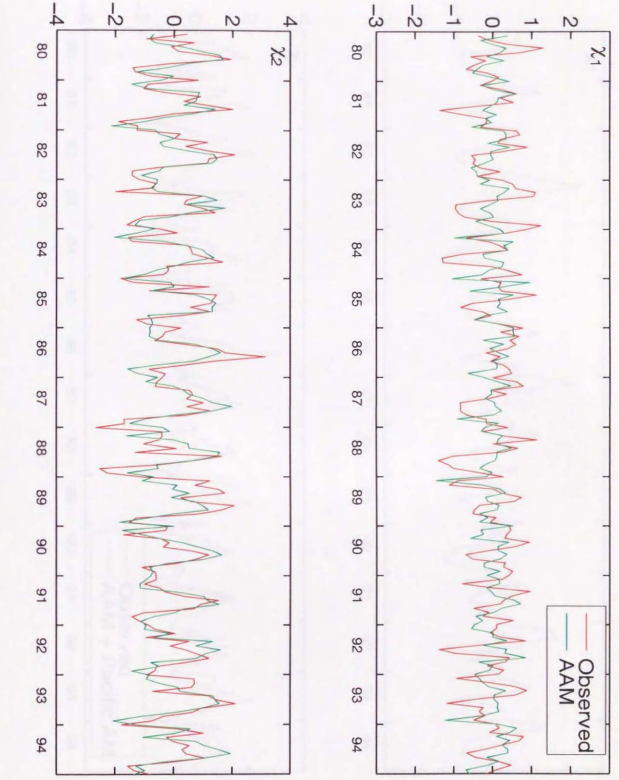

Figure 4.2: Red for Observed, Green for NCEP AAM. Vertical Unit is 10^{-7} rad. Long term trend is removed with four degree polynomials.

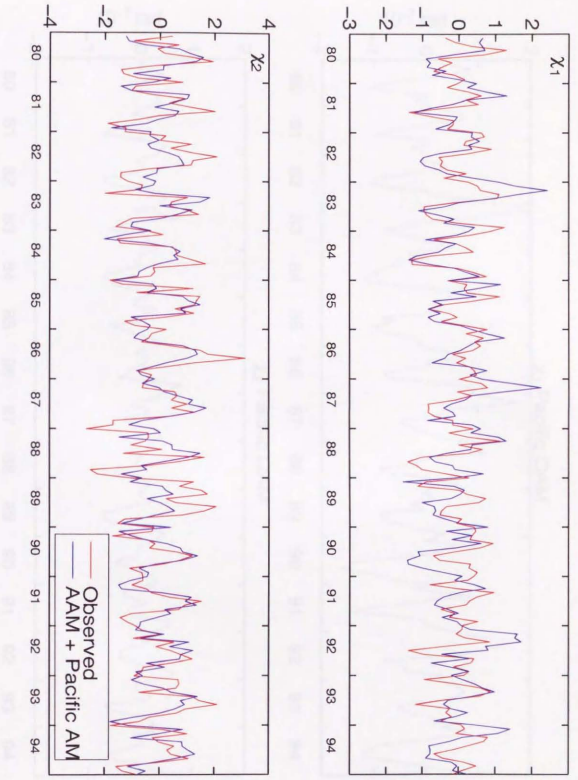

Figure 4.3: Red for Observed, Blue for NCEP AAM plus Pacific OAM. Vertical Unit is 10^{-7} rad. Long term trend is removed with four degree polynomials.

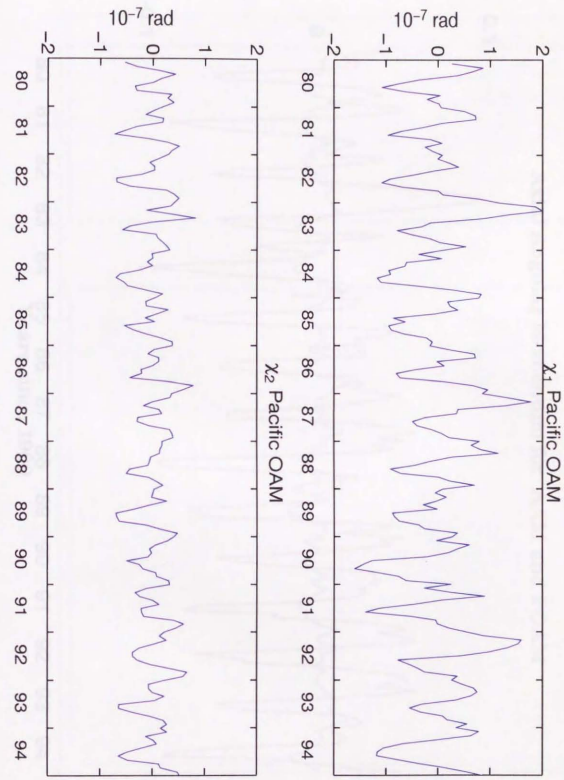

Figure 4.4: Pacific ocean angular momentum after the removal of long term variation fitted with four degree polynomials. Horizontal axis represents year after 1900.

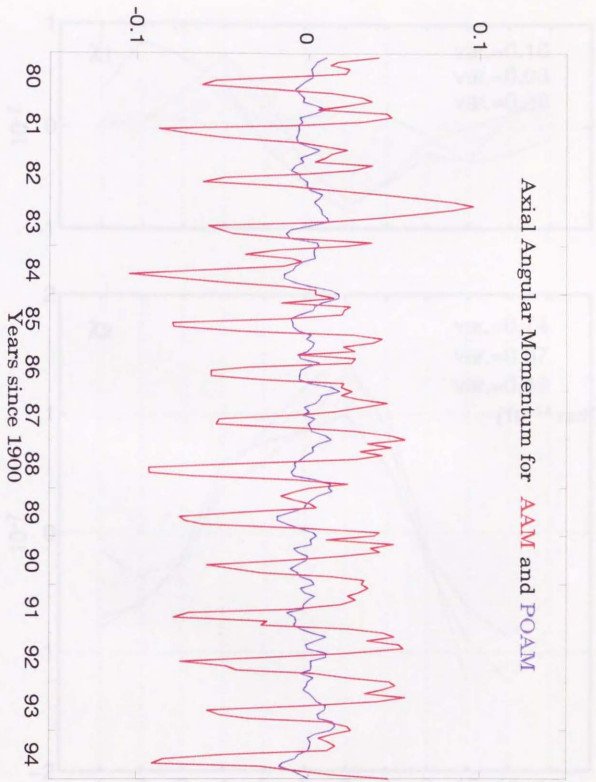

Figure 4.5: Axial angular momentum for AAM(red) and Pacific contribution (blue) after the removal of long term variation fitted with four degree polynomials. Horizontal axis represents year after 1900. Vertical unit is 10^{-7} radian.

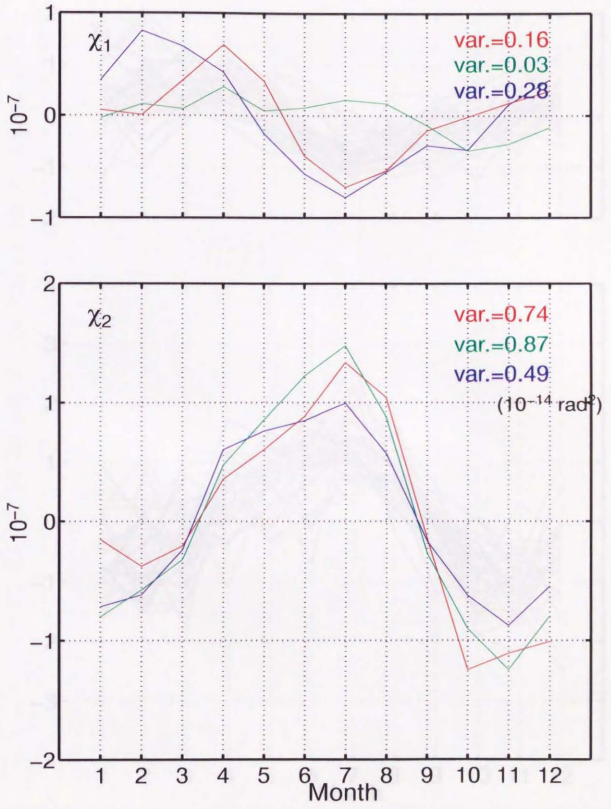

Figure 4.6: Mean yearly excitations for inferred (red), AAM (green) and AAM plus POAM (blue). The variance of each component is indicated.

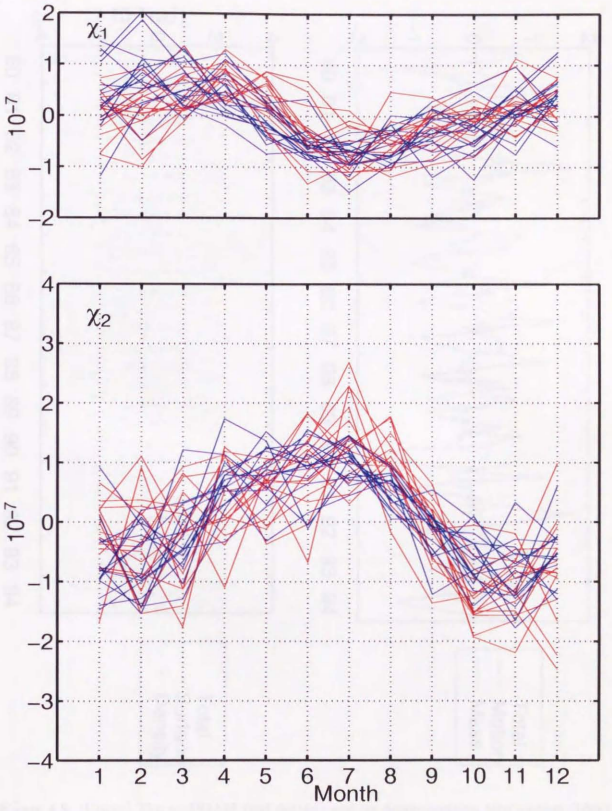

Figure 4.7: Yearly excitations of 15 years for inferred (red) and AAM plus POAM (blue). We can see the amount of year to year fluctuation.

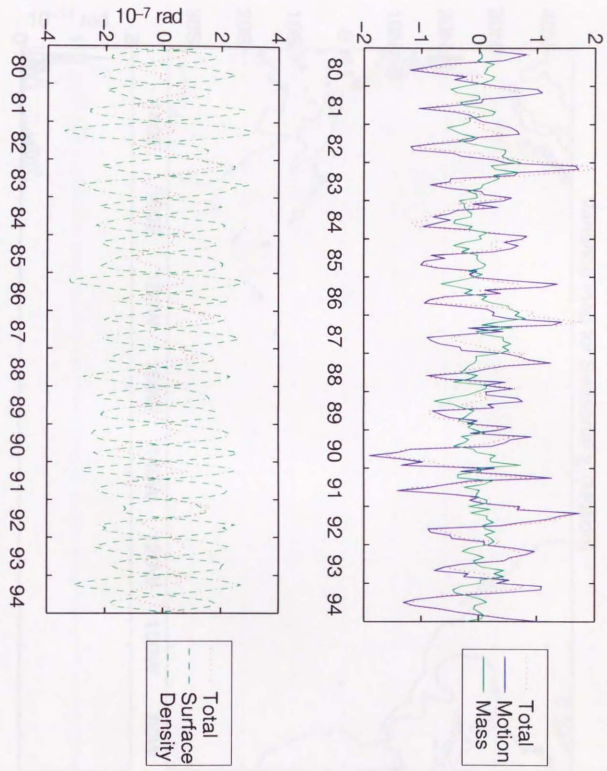

Figure 4.8: [Upper] The χ_1 POAM (red dotted) and its decomposition into motion (blue) and mass (green) term. [Lower] The mass term above is further decomposed into contribution from sea-surface(dashed) and density(dash-dotted) fluctuation.

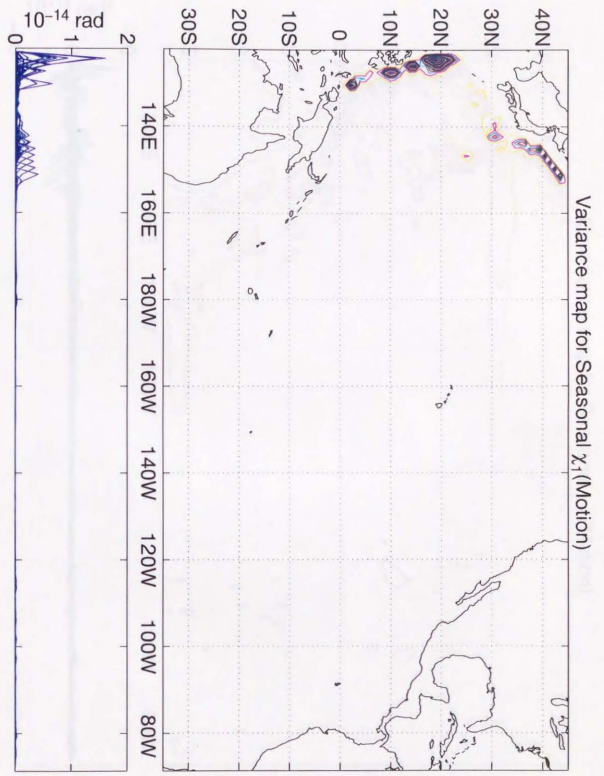

Figure 4.9: Variance map for Seasonal Pacific ocean angular momentum variation in χ_1 motion term (Top), and its cross section at each latitude (Bottom).

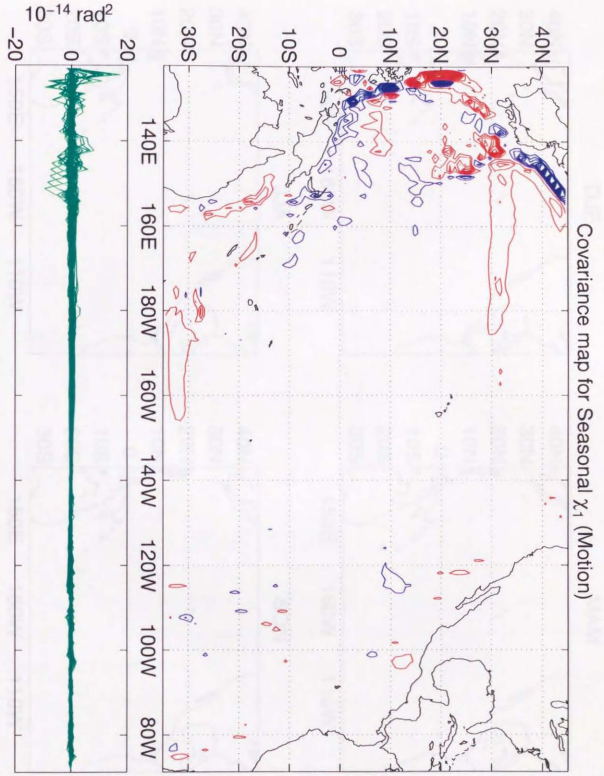

Figure 4.10: Covariance map for Seasonal Pacific ocean angular momentum variation in χ_1 motion term (Top), and its cross section at each latitude (Bottom). Top: Positive values are in red, negetive in blue.

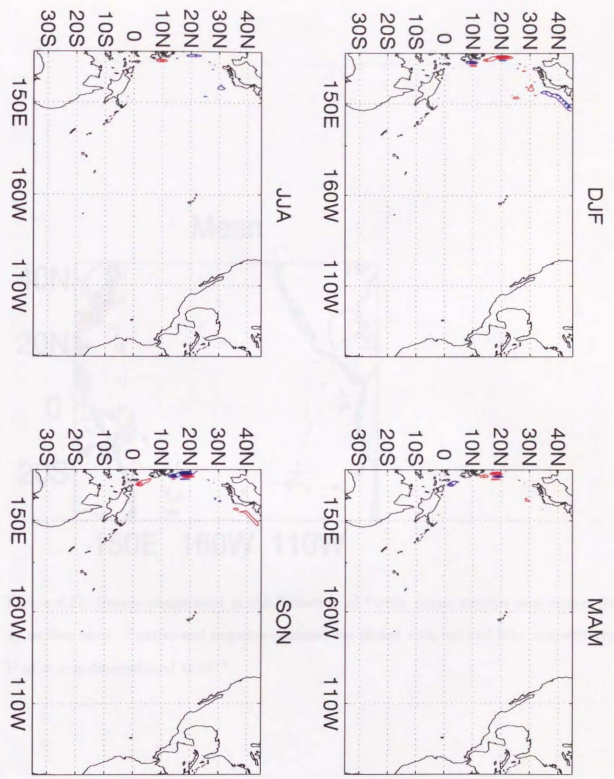

Figure 4.11: Seasonal Variation of Pacific ocean angular momentum for χ_1 motion term. Positive and negative contours are ploted with red and blue, respectively. Unit is non-dimenstional in 10^{-9}.

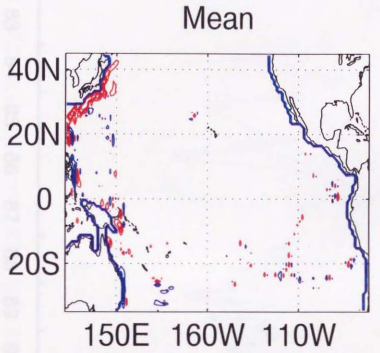

Figure 4.12: Steady component in the Variation of Pacific ocean angular momentum for χ_1 motion term. Positive and negative contours are ploted with red and blue, respectively. Unit is non-dimenstional in 10^{-9}.

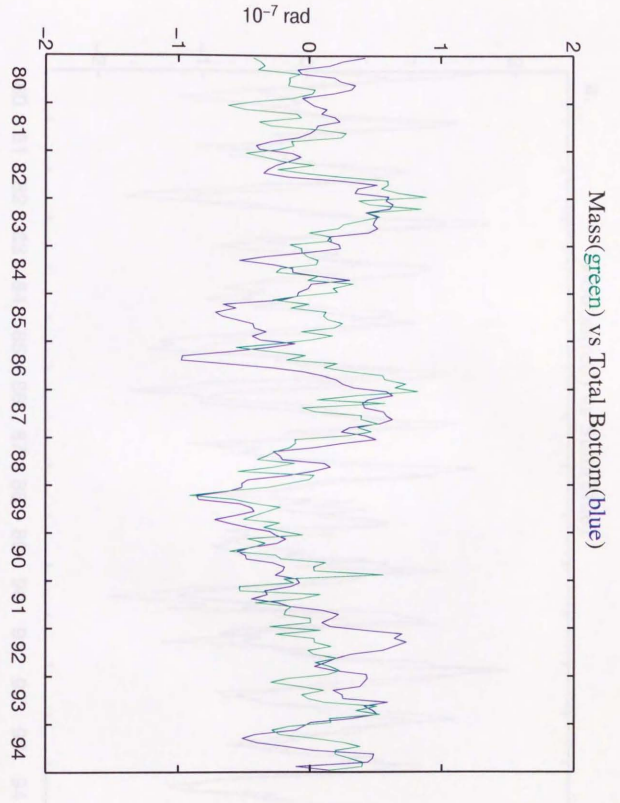

Figure 4.13: Mass(green) and Total–Bottom pressure(blue) term for χ_1 component. The bottom pressure term acting upon the sea floor topography is the difference, blue – green.

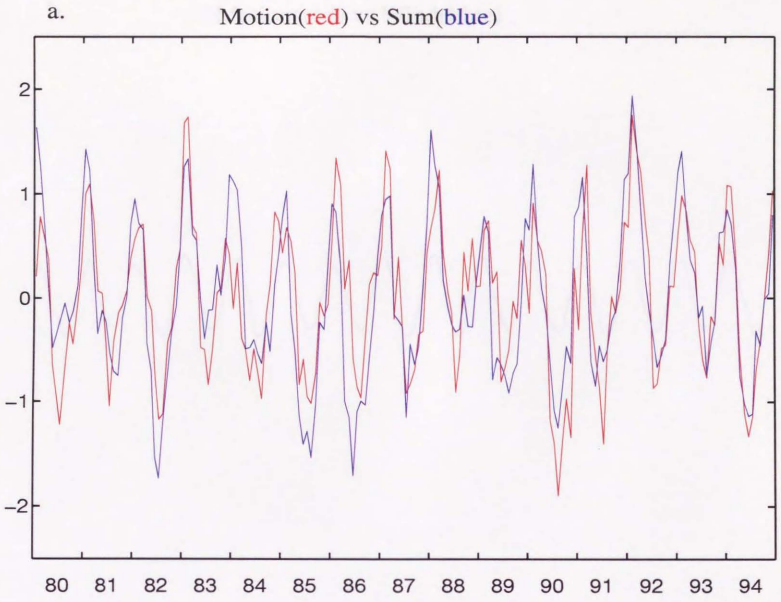
a.
Motion(red) vs Sum(blue)
2
1
0
−1
−2
80
81
82
83
84
85
86
87
88
89
90
91
92
93
94

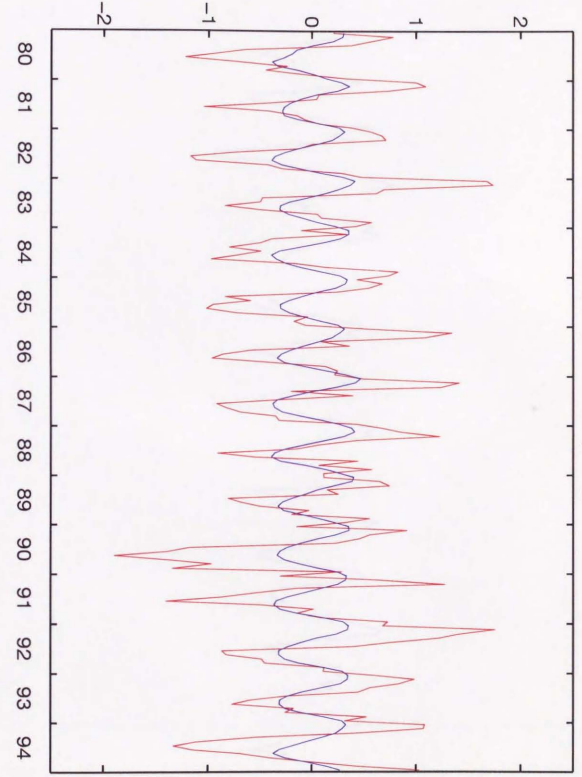
b.
Motion(red) vs Wind(blue)
2
1
0
−1
−2
80
81
82
83
84
85
86
87
88
89
90
91
92
93
94

c. Motion(red) vs Friction(blue)

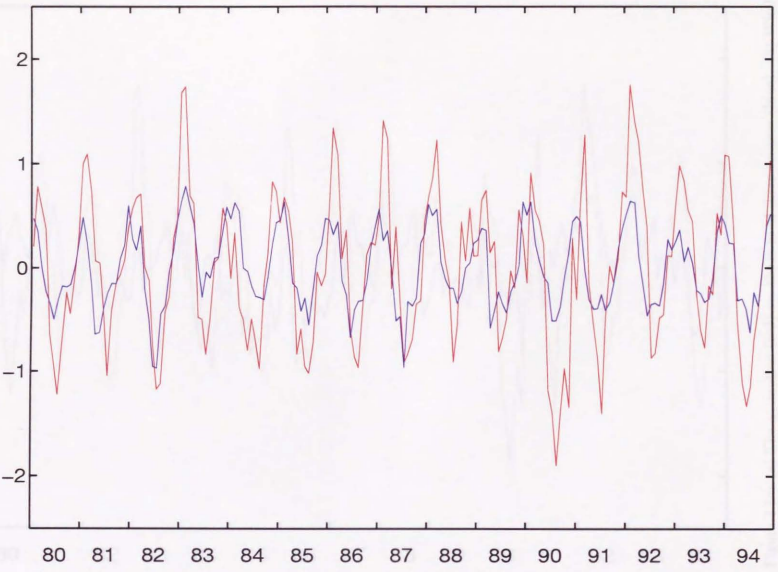

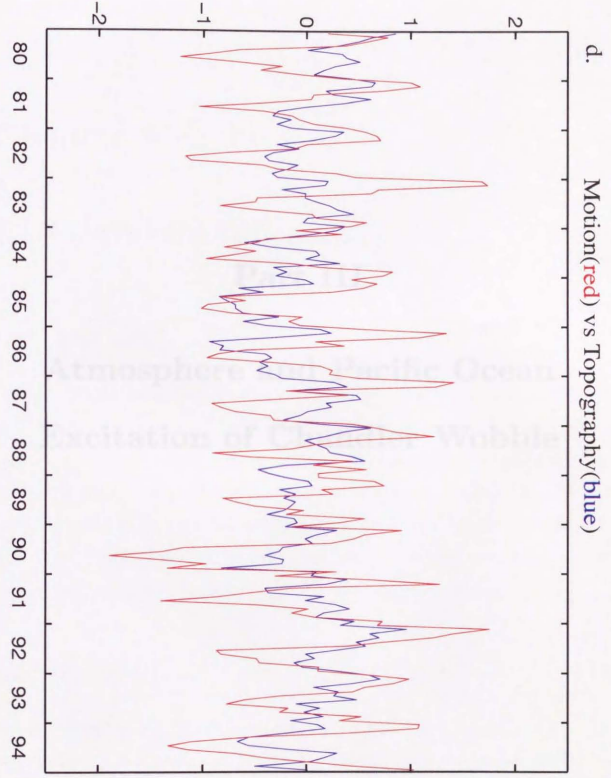

Figure 4.14: (a) The χ_1 motion (red) vs. the sum of three torques (blue). (b) Wind stress torque (blue). (c) Friction torque (blue). (d) (Sea floor) topography torque (blue). The vertical unit is non-dimensional, 10^{-7}, and the horizontal axis denotes years after 1900.

Part III

Atmosphere and Pacific Ocean Excitation of Chandler Wobble

Chapter 5

Atmospheric Influence

5.1 Abstract

The monthly global atmospheric reanalysis data by U. S. National Center for Environmental Prediction(NCEP) are used to examine the atmospheric contribution to the excitation of Chandler wobble(CW) for the period, 1979–1995. The spectral analysis tells that the atmospheric power is marginally comparable to the required one to excite CW, while the wobble domain analysis shows that the atmospheric contribution accounts about the half of the observed wobble amplitude. Examining the relative importance of pressure and wind term, we confirmed that the wind contribution is larger than that of pressure one.

5.2 Introduction

Variation of the Earth's spin axis with respect to the figure axis is known as wobble. It mainly consists of two components; the annual wobble (AW) and Chandler wobble (CW) [*Munk and MacDonald*, 1960; *Lambeck*, 1980; *Eubanks*, 1993]. The Earth's wobble is the result of excitations and provide us information about Earth's deformational response properties well below the seismic band. Improved understanding of Earth's response will

come with knowledge of the excitations. AW is presumably excited by the atmosphere [e.g., *Wilson and Haubrich*, 1976; *Wahr*, 1983; *Chao and Au*, 1991], land water [e.g., *Chao and O'Connor*, 1988; *Kuehne and Wilson*, 1991] and the ocean [e.g., *Wahr*, 1983; *Salstein et al.* 1995; *Steinberg et al.* 1995] although the budget is still not closed.

Though the excitation of CW has remained elusive over the past century, the recent studies suggest that atmospheric contribution plays an important role [e.g., *Kuehne et al.* 1993; *Chao*, 1993] (see, for a review, e.g., *Munk and MacDonald*, 1960; *Lambeck*, 1980; *Eubanks*, 1993). However, as pointed out in *Furuya et al.* [1996], *Kuehne et al.* [1993] and *Chao* [1993] do not focus their attention to the vicinity of Chandler eigen frequency around which the CW is most effectively excited. Even if the atmospheric pressure term well accounts for the rapid-wobble with intra-seasonal frequencies, it remains uncertain whether or not the pressure term dominates over the wind term around Chandler frequency. Looking into the vicinity of Chandler frequency, *Brzezinski* [1995] and *Furuya et al.* [1996] argue the importance of wind contribution. Moreover, *Furuya et al.* [1996] suggested that the CW is excited by quasi-periodic wind signal rather than excited randomly.

The purpose of this paper is to revisit our former result on the wind excitation of CW, employing newly implemented atmospheric data by U. S. National Center for Environmental Prediction (NCEP). A detailed discussion on the data sources is skipped, for they are described in section 3.4. We carry out several types of analyses, the conventional spectral analysis (section 5.3.1) and the wobble domain analysis (section 5.3.2). In section 5.3.3, we examine the atmospheric regional contribution in the same way as we did in Chapter 3. In addition, we investigate the possible region where the unaccounted signal(s) can reside, by changing the conventional coordinate axes (section 5.3.4 and 5.3.5). Summary is given in section 5.4.

5.3 Method and Results

5.3.1 Spectral Analysis

We compare the spectrum of observed and AAM excitations in order to grasp a broad band feature of AAM and the inferred excitation. The power spectrum is computed in terms of multi-taper techniques [*Thomson*, 1982; *Parcival and Walden*, 1993].

The observed excitation is inferred by deconvolving the wobble data, SPACE95 [see, *Gross*, 1996], with prescribed Chandler period and Q of 434 days and 100, respectively [e.g., *Wilson and Vicente*, 1990; *Furuya and Chao*, 1996]. In the deconvolution, we employed the Wilson's simplest filter [*Wilson*, 1985]. Since SPACE95 is daily data set, the phase distortion associated with numerical deconvolution is negligible. The daily observed excitation is averaged into monthly averaged values, in order to accommodate with monthly NCEP AAM series.

The non–seasonal variation of both observed and AAM excitation is computed, by removing long term variation as well as seasonal term, after fitting with the three-degree polynomials plus annual sinusoid with its higher harmonics up to 4 times annual frequency. In principle, we would like to know how broad is the peak of annual signal, since the broadness may account for the Chandler wobble excitation. Surely, the annual peak shows broad feature. However, we will not know whether the broad peak is caused by reality or spectral leakage; the latter is inevitable because of both a high dynamic range due to the annual signal and a finite length of data.

Results are shown in Figure 5.1. As discussed in *Furuya et al.* [1996], the AAM power is marginally comparable in the vicinity of Chandler frequency, whereas its power is generally smaller than that of observed excitation over wide frequency band. Figure 5.1 clearly shows that wind AAM is far from negligible, and that it acts to increase the AAM excitation power. As for the relative importance of pressure and wind term near the Chandler frequency, the power level of both term is marginally comparable to each other (Figure 5.1).

Figure 5.2 shows, however, that wind term is important compared with pressure term; these results are consistent with those described in *Furuya et al.* [1996]. However, we do not clearly observe a spectral peak near the Chandler band which was suggested from JMA wind AAM in *Furuya et al.* [1996], and thus we could not strengthen their suggestion.

5.3.2 Wobble Domain Analysis

Next, in order to examine the atmospheric power near the prograde Chandler frequency, we will employ the wobble domain analysis. We revitalized this method in *Furuya et al.* [1996; submitted to *J. Phys. Earth*], although it has once been criticized [*Chao*, 1985]. The discussion in *Chao* [1985] is a correct criticism as long as one's integration is started with non-zero initial values; totally different two excitations can yield similar two wobbles if the integration is started out with the same initial value, due to the freely decaying CW. However, by integrating the non–seasonal excitation obtained above with zero initial value, one can shed light on the excitation power near eigen frequency; we can get rid of signals unimportant for Chandler wobble excitation.

Besides starting the integration with zero initial value, it is also very important to totally reject seasonal signals. This is because, if the seasonal signals are involved, it can yield both annual and Chandler wobble in the transient stage of integration; as long as the Q value is 100, it would take more than three decades to arrive at steady state. To obtain the non-seasonal excitation, after computing an averaged annual cycle composited 17 years of data, we removed it from the trend-removed excitation every year. The integration is performed with the same Chandler period and Q as those used in the deconvolution above. The results shown below are restricted only to the period from 1980–1994, to compare the ocean contribution discussed in Chapter 6, but are not essentially altered even if we analyze from 1979–1995.

Figure 5.3 shows the result. In view of the absence of 6 year beating phenomena in

Figure 5.3, we are convinced of the rejection of seasonal signals. The agreement is not very good, while both wobbles are almost in phase with each other. The standard deviation of AAM-induced wobble is 47 % of that for observed wobble. Thus, the observed wobble cannot be explained only in terms of NCEP AAM. Shown in Figure 5.4 are the wind and pressure contributions for AAM-induced wobble in Figure 5.3. As a result, the standard deviation of wind-induced wobble is 33 % larger than that for the pressure induced wobble. Hence, the wind term is far from negligible, and rather plays a dominant role in atmospheric Chandler wobble excitation as pointed out by *Brzezinski* [1995] and *Furuya et al.*, [1996].

In view of the observed wobble in Figure 5.3, we recognize a linearly growing amplitude, which is observed in the case of 'resonant' Chandler wobble excitation [*Furuya et al.*, 1996; submitted to *J. Phys. Earth*]. This implies an existence of coherent signal near the Chandler frequency, i.e., some 14 months' variability. Although we described that JMA wind AAM contains such a signal [*Furuya et al.* 1996], the wind-induced wobble in Figure 5.4 does not unambiguously reveal such a feature. Thus, we are led to recognize that the existence of 14 months' periodic wind signal is still marginal.

5.3.3 Regional Contribution

The regional atmospheric signal which can potentially excite the Chandler wobble is examined. For this purpose, we compute 14 months–stacked excitation, which we regard as a proxy of the excitation signal of Chandler wobble. It is true that the CW is not necessarily excited periodically as is the case of AW. Nevertheless, the stacking procedure will get rid of unimportant signals for excitation of CW, since the CW is most efficiently excited by signals around eigen frequency when considered in frequency domain. Moreover, *Furuya et al.* [1996] suggests the possibility of resonant excitation by atmospheric wind, although it is not strengthened from the spectral analysis in this paper.

Both the data and analysis method are almost the same as those in our study on the at-

mospheric annual wobble excitation (Chapter 3). At the outset, we compute non–seasonal gridded AAM spanning over 17 years, by subtracting the seasonal variation at each grid which is computed by stacking the gridded AAM at the same month over 17 years[1]. Summing up the whole gridded AAM at each month for each term[2], we compute the non–seasonal global AAM[3]. Next, we divide the whole non-seasonal series into several segments with each length of 14 months; since the whole data set spans 180 months, we have to reluctantly take away the left-over. Afterward, we stack them to obtain the mean 14 months-excitation. We will treat this 14 months' excitation in the same way as we did for seasonal excitation. It is to be noted, however, that the signal to excite the Chandler wobble resides near the *prograde* frequency, and that the *retrograde* signal is also included in the time series. Even so, the following analysis will tell where is particularly important for the atmospheric contribution to the excitation of CW.

Shown in Figures 5.5 and 5.6 are regional variance for the 14 months' stacked pressure and wind AAM, respectively. Figure 5.5 shows that the pressure variation is localized over north-western Eurasian continent as well as over the north America. The variance is smaller than that for wind term in view of Figure 5.6. The most intensive fluctuation in the 14 months' wind term originate in the north-eastern Atlantic and north-eastern Pacific. The variance itself is significantly larger than that for the pressure term in Figure 5.5.

The two figures 5.5 and 5.6 simply illustrate where the fluctuation is energetic, and do not indicate how the regional variation contributes to globally integrated (total) AAM and wobble excitation. Figures 5.7 and 5.8 show the covariance between regional variation and the total pressure and wind AAM, respectively. Figure 5.7 tells that the two intensive

[1]This procedure is carried out with my own MATLAB m-file (rns.m)

[2]This is done by my own MATLAB m-file (ncep_nsmk.m)

[3]The non–seasonal global AAM computed in this way is not exactly the same as those computed by simply subtracting the long-term trend and seasonal term, since the m-file(ncep_nsmk.m) does not remove long term trend. However, as long as the attention is paid around annual signal, i.e., 14 months' signal, the difference will have little influence on the results below

regions noted above vary in a in–phase manner. On the other hand, the total wind term does not consist of any polarized area (Figure 5.8). Comparing Figures 5.6 and 5.8, the the north-eastern Atlantic contribute positively to the total wind term, while the fluctuation over the north-eastern Pacific cancels the total wind term. Figure 5.8 indicates that the wind term consists of complex regional pattern, and that it is not as simple as the case for Figures 5.5 and 5.7.

Next, we investigate the covariance between regional variation and the observed excitation. Results are shown in Figures 5.9, 5.10 and 5.11. In view of Figure 5.9, the contribution pattern over the two extensive regions is different from that indicated in Figure 5.7: the variation over the northwestern Eurasia is out of phase with the observed excitation. The seemingly inconsistent pattern depicted in Figures 5.7 and 5.9 can be reconciled, however, by taking a look at Figures 5.10 and 5.11. We can clearly recognize the similarity between Figure 5.10 and 5.11. It illustrates that the wind contribution is rather important than the pressure contribution for the observed excitation.

The present analysis on atmospheric regional contribution to the CW excitation also supports the importance of wind term. It is interesting that the northeastern Atlantic region is close to the North Sea area, where the enhanced non–equilibrium pole tide has been observed: recent researches suggest that it is a periodically forced phenomena by atmospheric wind [e.g., *O'Connor*, 1986; *Tsimplis et al.* 1994: but see also *Xie and Dickman*, 1995].

5.3.4 Agreement viewed from modified axes

In Chapter 3 and 4, we analyzed the seasonal wobble excitation, viewing the two-dimensional excitation from X–(toward 90 deg. W longitude) and Y–(toward Greenwich meridian) axis. Since the χ_2 component could be well explained by atmospheric pressure term, we could shed light on the discrepancy originating in the torque around X-axis. However, it was

simply fortuitous that we could immediately move on the χ_1 component, because the conventional axes orient toward such two directions. Prompted by those results, we carry out the following analysis in order to provide a constraint on the possible unaccounted sources for the CW excitation.

Figure 5.12 illustrates how the stacked 14 months' excitation pole (magnified by 150) moves around North pole for both observed (red) and AAM (blue) excitation. At first glance, both excitations have comparable amplitude, and polarize toward similar orientation. Figure 5.13 shows the contribution from pressure (green) and wind (blue) term. The pressure term is larger than wind term in its amplitude, and causes the polarization in view of Figure 5.12. The variance of wind term, in turn, is smaller. Thus, the pressure term appears to be more important than wind term. However, we will show below that the better phase agreement is achieved mainly by the wind term; we can recognize in Figure 5.12 that the wind term also contribute to the polarization of stacked AAM excitation.

Decomposing two dimensional excitation pole into one dimensional time series, we examine the phase agreement between observed and AAM excitation (Figure 5.14a). In spite of the overall similarity shown in two dimensional Figure 5.12, the conventional coordinate axes in Figure 5.14a prevent appealing the agreement. Thus, we rotated the conventional axes by 33 degrees toward west, so that the best agreement between the observed and AAM (modified) is obtained for χ_2 component. Nevertheless, the correlation coefficient is 0.23, and this value itself is not significant (but see below). Based upon this modified axes, we examine the relative importance of wind and pressure. Results are shown in Figure 5.15. In light of the modified χ_2 in Figure 5.15, the correlation between the observed (red) and wind term (blue) is very good. The correlation coefficient is 0.52. If the degree of freedom is assumed to be $12(14-2)$, we can reject the null hypothesis with significance level of 0.1 that the wind term has no correlation with the observed excitation. On the other hand, the correlation coefficient between the observed and pressure term (green) is extremely low (-4.9×10^{-5}). Hence, as far as the modified χ_2 term is concerned, we conclude that the

wind term plays a major role.

5.3.5 Where does the remaining signal originate?

We modified the coordinate axes so that the best correlation is obtained in χ_2 component, and thus the correlation in the modified χ_1 term would be worse than that in original χ_1 of Figure 5.14a. However, we can take advantage of this result to constrain the area which can potentially explain the remaining signal.

The modified χ_2 represents a torque around the equatorial axis orienting toward 33 degrees' west longitude: hereafter, we call it X'-axis. So that, the modified χ_1 corresponds to the torque around the axis orthogonal to the X'-axis, and we call it Y'-axis: note that the positive Y'-axis orients toward 123 degrees' west longitude. Since the modified χ_2 can be well-explained by atmospheric wind as noted above, much of the remaining signal would be retained in the modified χ_1 component. Hence, first thing, we should consider such source(s) that can affect the torque around Y'-axis. The area which can have much influence on the torque will be the western Pacific, Philippine Sea and Atlantic ocean, since they are the furthest region from the Y'-axis and the angular momentum fluctuation over these area can contribute most efficiently to this torque. However, we do not claim that the Indian Sea is less important. Although the Philippine Sea and Atlantic data are not available at present, we will investigate the influence of the Pacific in a companion paper.

5.4 Summary

Atmospheric excitation of Chandler wobble is examined, using monthly NCEP reanalysis data which spans over 1979–1995, in order to confirm (or reject) the wind excitation hypothesis postulated in *Furuya et al.* [1996].

The results of spectral analysis show that the power is marginally comparable, and that the coherence is not significant. Although the NCEP AAM does not fully account for the

observed wobble, the wobble domain analysis illustrates the importance of wind signal. The existence of periodic excitation signal is implied in the observed wobble, but we could not confirm an existence of such signal in the NCEP AAM. Thus, we conclude that, although the NCEP AAM does not sufficiently account for the observed wobble, the wind term is more important than the pressure term. We could not observe a pronounced signal in the NCEP wind AAM around Chandler frequency.

We also implemented time–domain analysis in which the whole non–seasonal excitation series is stacked into 14 months' averaged series. Though this approach does not focus our attention to the prograde Chandler frequency, we could examine the regional contribution. The origin of pressure AAM term is localized over two continental area in the northern hemisphere. On the other hand, the wind AAM term does not originate in any specific area. It is certain, however, that the wind AAM around northeastern Atlantic fluctuates extensively, which may conform to the wind-stress origin hypothesis on the enigimatically enhanced North Sea pole tide.

By rotating the conventional coordinate axes about 30 degrees westward, the wind term around X'-axis, orienting toward 33 degrees west longitude, significantly correlates with the observed excitation. Moreover, we suggest that, based on this modified axes, the western Pacific, Philippine Sea and central Atlantic ocean would be an important area to explain the deficit of AAM for the observed excitation.

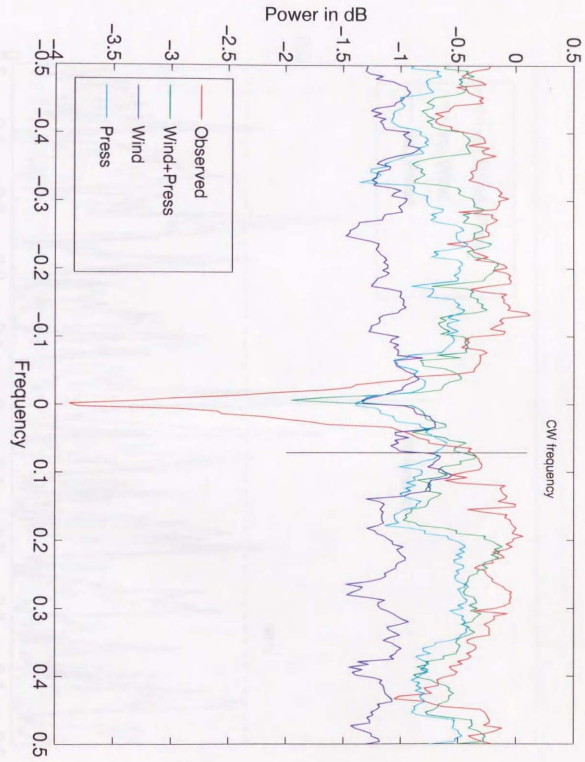

Figure 5.1: Power spectra for the non–seasonal excitations.

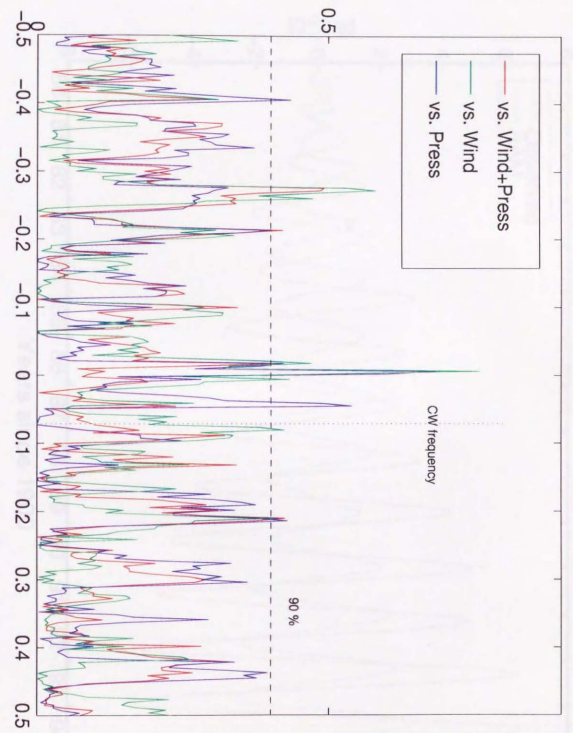

Figure 5.2: Coherence specta between non–seasonal observed and AAM excitations.

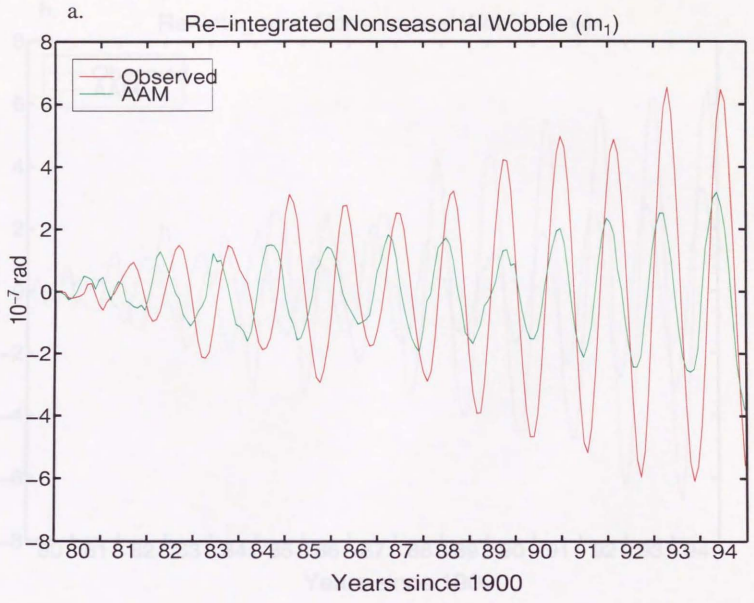
a.
Re–integrated Nonseasonal Wobble (m_1)
Observed
AAM
10^{-7} rad
8
6
4
2
0
−2
−4
−6
−8
80 81 82 83 84 85 86 87 88 89 90 91 92 93 94
Years since 1900

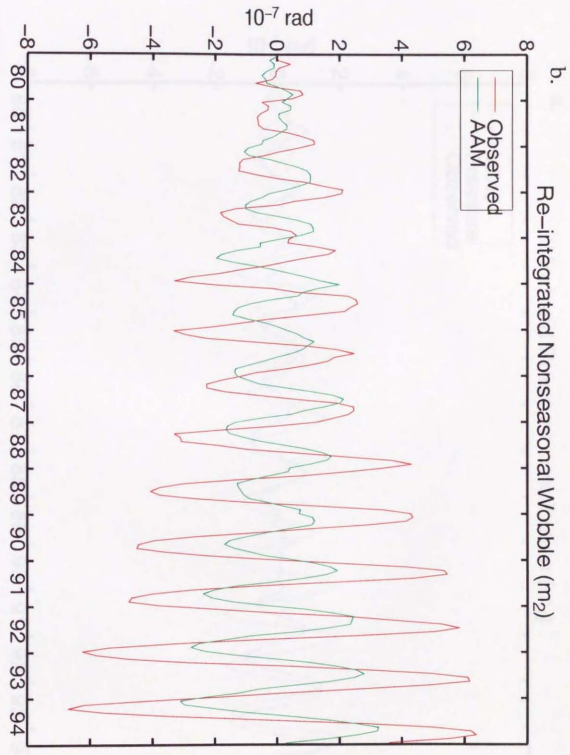

Figure 5.3: Recently excited non-seasonal wobble of the *observed* (red) and the AAM–induced (green) wobbles, where the Chandler period and Q–value are 434.0 days and 100, respectively. (a) m_1 (b) m_2 component.

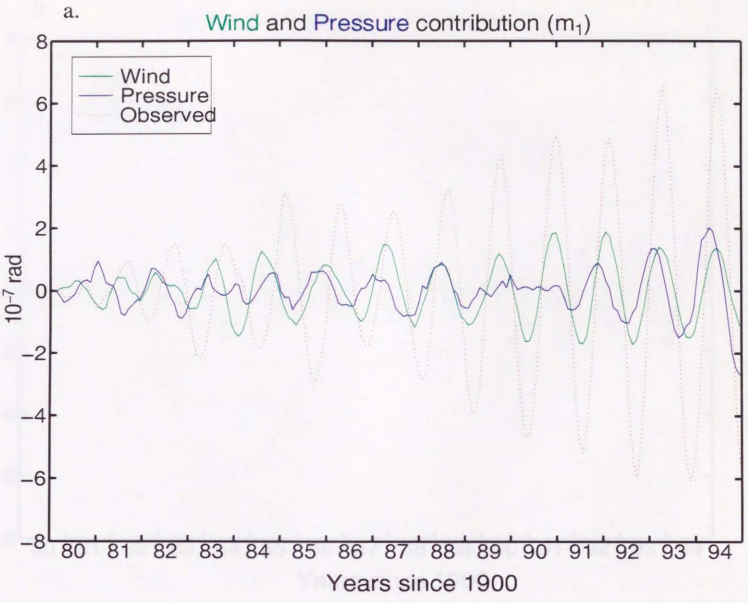
a.
Wind and Pressure contribution (m_1)
Wind
Pressure
Observed
10^{-7} rad
8
6
4
2
0
−2
−4
−6
−8
80
81
82
83
84
85
86
87
88
89
90
91
92
93
94
Years since 1900

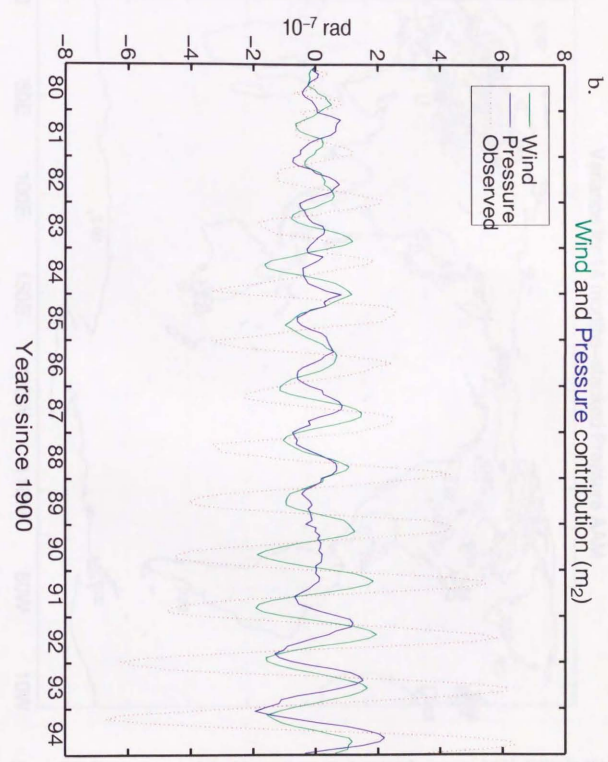

Figure 5.4: Wind (green) and pressure (blue) contributions to the AAM- induced wobble. Red-dotted line denote observed wobble, which is the same in the previous figure. (a) m_1 (b) m_2 component.

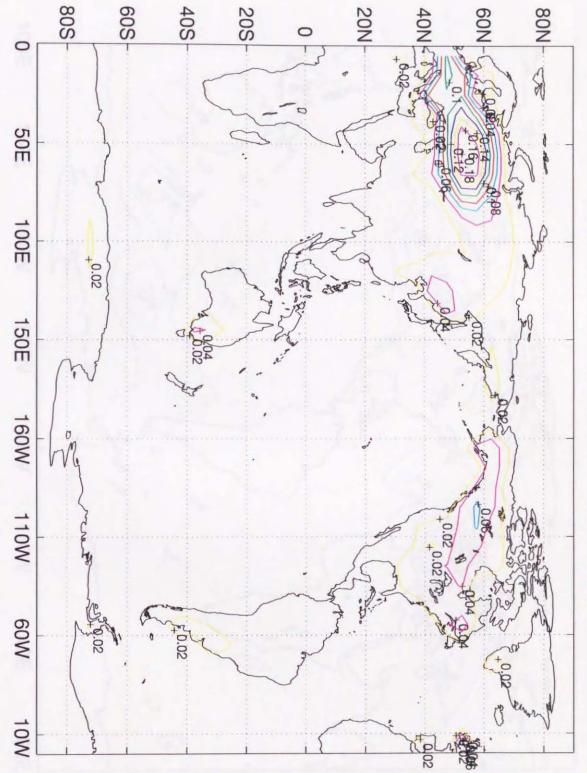

Figure 5.5: Variance map of the 14 months stacked regional pressure AAM. Units in 10^{-20} (rad^2).

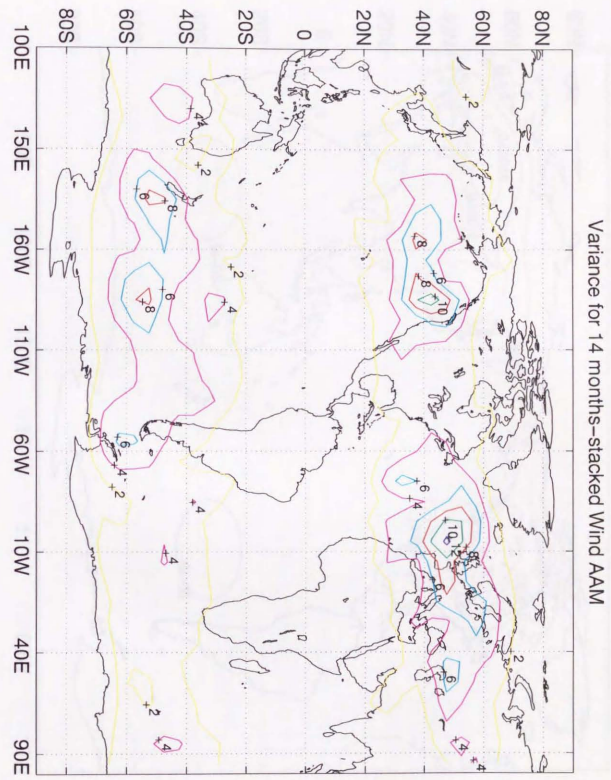

Figure 5.6: Variance map of the 14 months stacked regional wind AAM. Units in 10^{-20} (rad^2).

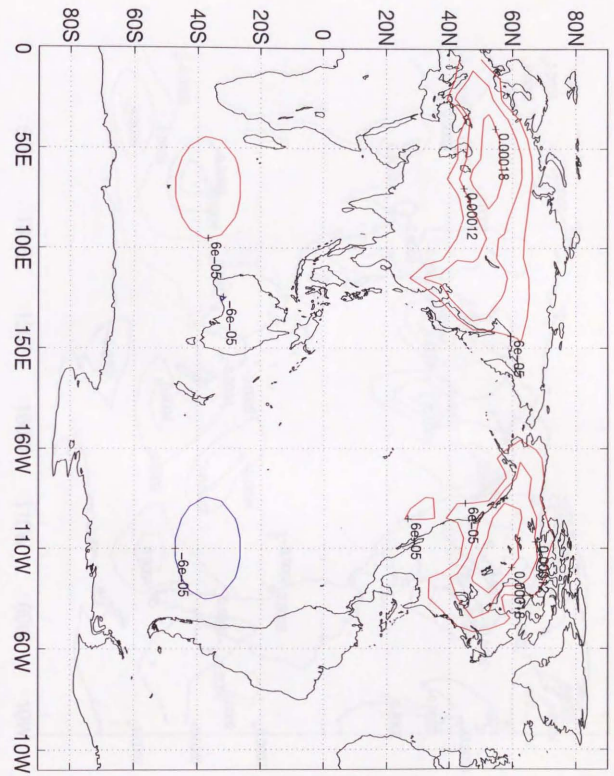

Figure 5.7: Covariance map of the 14 months stacked regional pressure AAM. Units in 10^{-20} (rad^2).

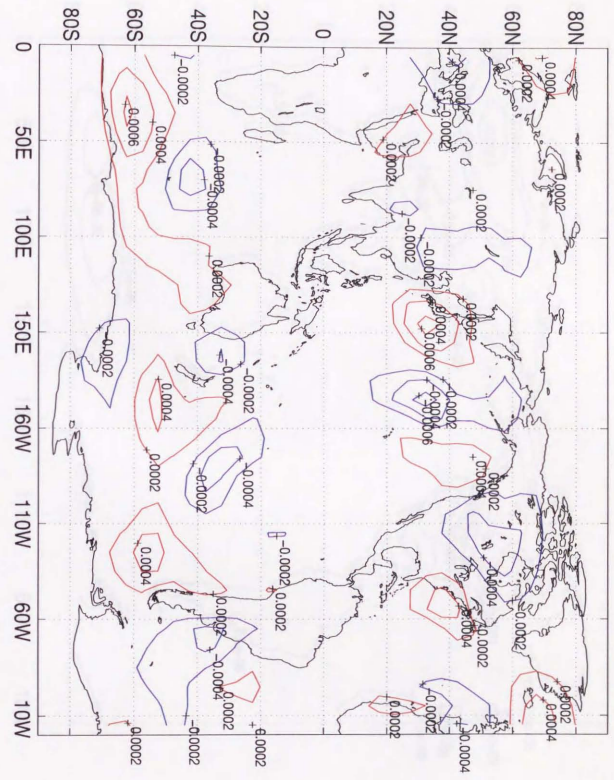

Figure 5.8: Covariance map of the 14 months stacked regional wind AAM. Units in 10^{-20} (rad^2).

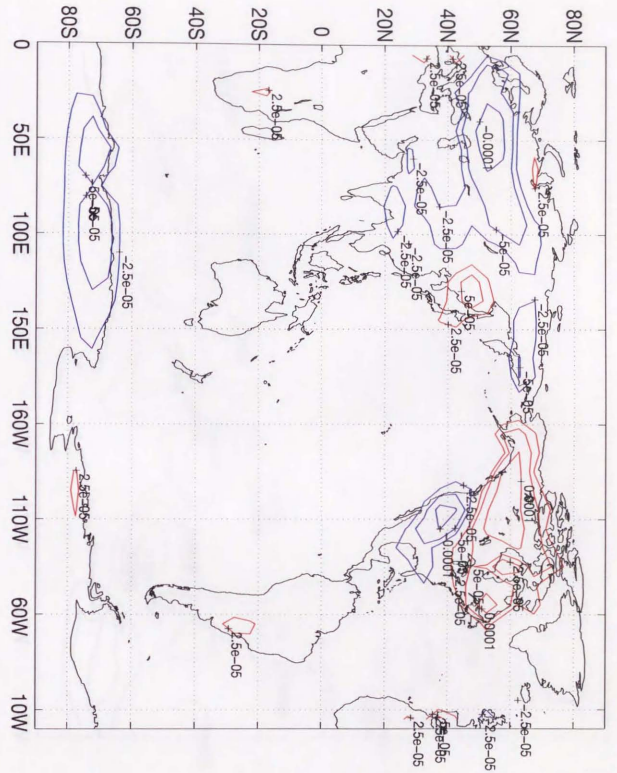

Figure 5.9: Covariance between the 14 months stacked pressure AAM and the observed stacked excitation. Contour intervals are .000025 .00005 .0001 for positive(red), and -.000025 -.00005 -.0001 for negative(blue) covariance.

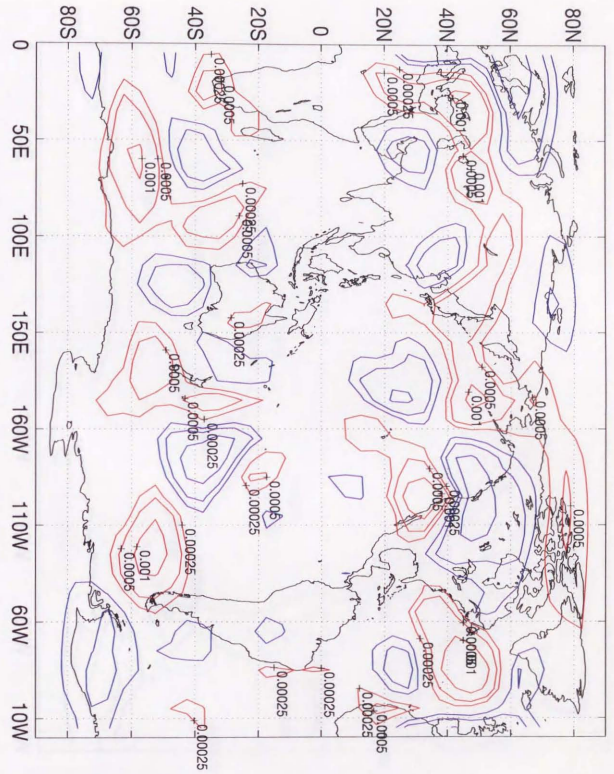

Figure 5.10: Covariance between the 14 months stacked wind AAM and the observed stacked excitation. Contour intervals are .00025 .0005 .001 for positive(red), and -.00025 -.0005 -.001 for negative(blue) covariance.

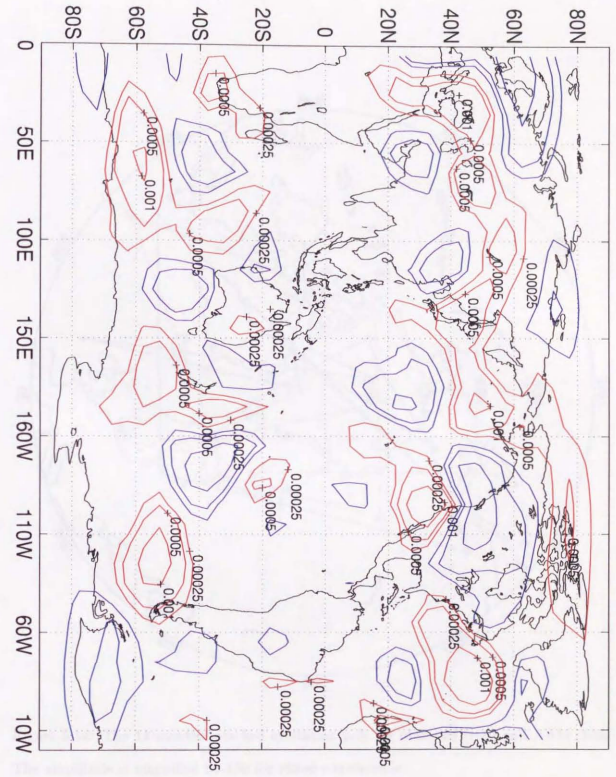

Figure 5.11: Covariance between the 14 months stacked wind plus pressure AAM and the observed stacked excitation. Contour intervals are .00025 .0005 .001 for positive(red), and -.00025 -.0005 -.001 for negative(blue) covariance.

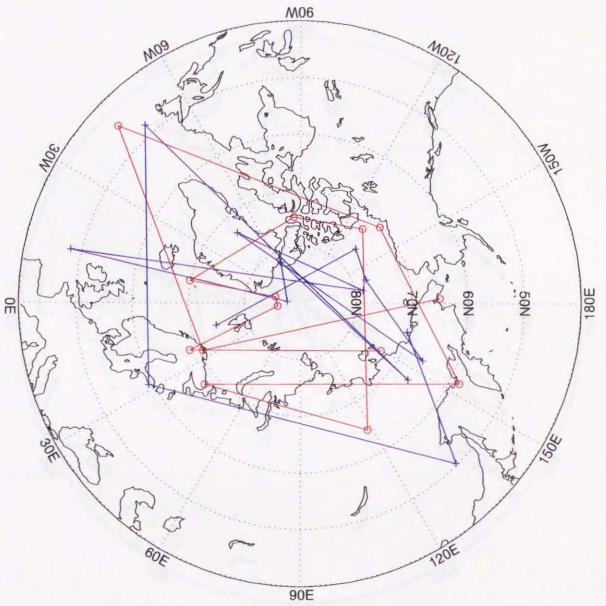

Figure 5.12: The 14 months' stacked excitation pole for observed (red) and AAM (blue). The amplitude is magnified by 150 for visual convenience.

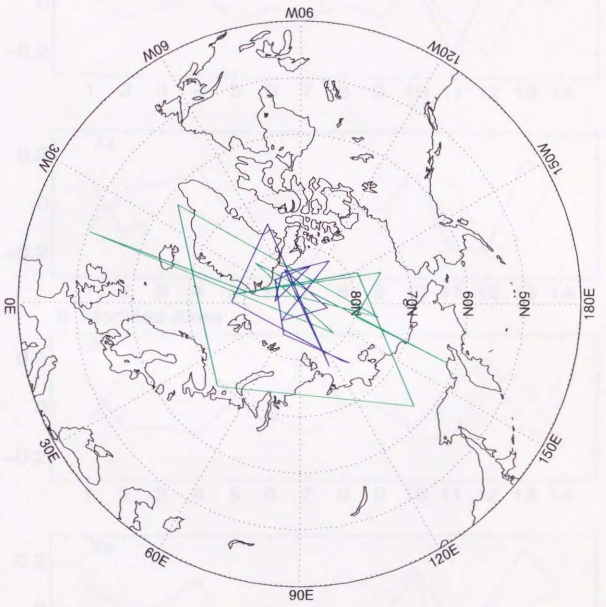

Figure 5.13: Green for pressure term and blue for wind term.

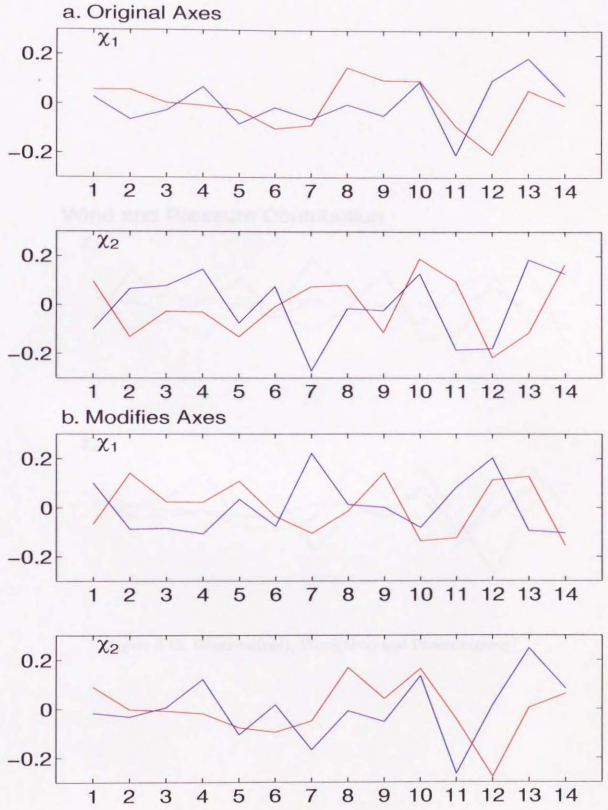

Figure 5.14: Observed(red) and AAM(blue)

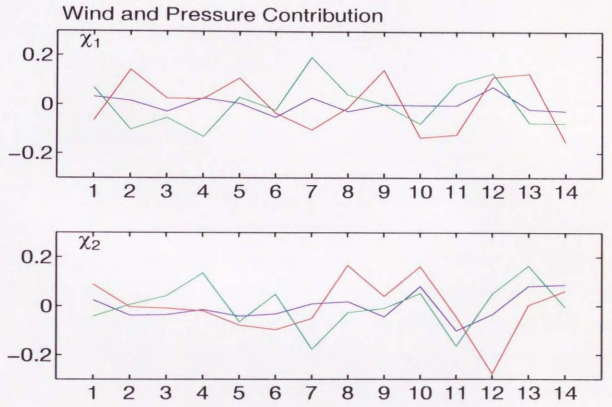

Figure 5.15: Observed(red), Wind(blue) and Pressure(green)

Chapter 6

Pacific Ocean Influence

6.1 Introduction

Using the NCEP reanalysis data, we indicated in a companion paper that the wind contribution dominates over the pressure induced wobble, and that the 14 months' stacked wind atmospheric angular momentum (AAM) around modified X'-axis significantly correlates with the corresponding observed excitation: these results for the importance of wind are consistent with the recent results by *Brezezinski* [1995] and *Furuya et al.* [1996]. However, it is also to be noted that the NCEP AAM does not totally explain the observed Chandler wobble excitation. Moreover, though the observed wobble suggested a 'forced' excitation by 14 months' periodic signal, the AAM excitation did not.

Meantime, using the NCEP ocean analysis data [see, *Leetmaa and Ji*, 1989; *Ji et al.* 1994; *Ji et al.* 1995], we showed that the Pacific ocean current contribution accounts for χ_1 component of annual wobble excitation which the AAM could not explain. The implications of the result are three folds: (i) oceanic contribution cannot be ignored for the excitation of Earth's wobble; (ii) the ocean analysis data, independently obtained from Earth rotation observation, have a sufficient quality to study its influence on the Earth's variable rotation; (iii) by rotating the conventional coordinate axes, we can illuminate the

areas in which unaccounted signals may originate. Since the χ_2 component turned out be fortunately well-explained by AAM alone, we could shed light on the χ_1 term in which much of the discrepancy is involved. The χ_1 term represents a torque around 90degE longitude axis, and it geographically captures the Pacific Ocean contribution. Hence, we studied the Pacific Ocean contribution, not only because of its large area.

The analysis below is motivated by our conjecture in Chapter 5 that the far western Pacific and central Atlantic would be potentially important region to account for the remaining discrepancy. However, since the NCEP ocean analysis data publicly available is confined only to the Pacific, the purpose of this paper is to examine the influence of Pacific Ocean on Chandler wobble excitation.

6.2 Data

The data sets used here is the same as those in Chapter 3, 4 and 5. For polar motion data, see *Gross* [1996]. For NCEP reanalysis data, see *Kalnay et al.* [1996]: for the formulation of AAM, contact *Barnes et al.* [1983]. For ocean analysis data, see *Leetmaa and Ji* [1988], *Ji et al.* [1994] and *Ji et al.* [1995]. The computation of Ocean angular momentum is described in Chapter 4 at length [see also, *Ponte and Rosen*, 1994].

6.3 Results

The following analysis is carried out for the 15 years period, 1980–1994, during which the monthly NCEP ocean analysis data is available.

6.3.1 Spectral Analysis

In this section, we compare the spectrum of non-seasonal observed, AAM and Pacific OAM excitations in order to examine the influence of Pacific OAM for the Chandler wobble

excitation. As in Chapter 5, the power spectrum is computed in terms of multi-taper techniques [*Thomson*, 1982; *Parcival and Walden*, 1993].

At the outset, we obtain the non-seasonal variation from the observed excitation, AAM and Pacific OAM. In computing the observed excitation, the Chandler wobble period and Q are prescribed to be 434 days and 100, respectively [e.g., *Wilson and Vicente*, 1990; *Furuya and Chao*, 1996]. We removed seasonal variation and its higher harmonics up to four times annual frequency as well as long-term variation (assumed to be three degree polynomials). The non-seasonal excitation series are shown in Figure 6.1 and 6.2: we illustrated them based on a modified axes described in Chapter 5 so that the best agreement could be achieved in the modified χ_2 component.

Since the results about non-seasonal AAM are discussed in Chapter 5 at length, we will put an emphasis on the influence of the Pacific Ocean on Chandler wobble excitation. The power spectrum estimates are shown in Figure 6.3. The power in the lowest frequency seen in AAM plus POAM is larger than that for AAM alone. We think that it is caused by the inter-annual component in the POAM (see Figure 6.2 and 6.4). However, considering the 95 % confidence level, the Pacific contribution does not significantly increase the power at much higher(intra-seasonal) frequencies. Figure 6.4 indicates that at higher frequencies the Pacific contribution is about 10 dB smaller than that of the atmosphere. Much of the Pacific Ocean contribution is confined into such frequencies lower than 0.15 cycle per year(6 months' period).

We examine the relative importance of current and mass term for the Pacific angular momentum in Figure 6.5. The current contribution dominates the mass redistribution effect over a wide frequency band. Thus, the torque acting on the Earth's ellipticity is small in Pacific excitation of Earth's wobble. This is to be contrasted with the atmospheric excitation in which the wind and mass contribution are comparable.

6.3.2 Wobble Domain Analysis

Figure 6.6 illustrates the result of wobble domain analysis as in Chapter 5 (see also, *Furuya et al.* [1996; submitted to *J. Phys. Earth.*]. As can be expected from Figure 6.3, the amplitude of Pacific induced wobble is much larger than that of AAM-induced wobble. At present, it is still open whether or not the global oceanic contribution can exceed the atmospheric power, since we do not take account for the contribution from other oceans. However, we could see that the oceanic angular momentum fluctuation is potentially important to excite the CW; Figure 6.6 indicates that we cannot ignore the ocean contribution for Chandler wobble excitation. The phase discrepancy is, however, appreciable; the Pacific-induced wobble is about 90 degrees forwarded by observed wobble. We speculate that the phase discrepancy may be explained by unaccounted ocean effects such as the Atlantic ocean.

The Pacific-induced wobble in Figure 6.6 consists of two constituents, i.e., current and mass redistribution effects as shown in Figure 6.7: the latter effect corresponds to the pressure term in AAM. The current contribution is larger than the mass redistribution effect, which conforms to the result in Figure 6.5.

6.4 Concluding Remarks

We examined the Pacific Ocean contribution to the excitation of CW, in order to investigate the potential importance of oceanic effect on the Earth's wobble; it is to be noted that the present analysis does not answer the question whether or not the global oceanic contribution will excite the CW.

When viewed over a broad frequency band, the Pacific ocean does not contribute to the wobble excitation so much at higher frequencies than 0.15 cycle per month (corresponding 6 months' period); at such frequencies, the non-seasonal AAM is about 10 dB larger than the non-seasonal POAM. Moreover, the current term dominates over the mass term over a

wide frequency band.

Taking a closer look around Chandler frequency, the POAM contribution far exceeds the global atmospheric contribution; this is confirmed by both spectral analysis and wobble domain analysis. The large contribution from the Pacific Ocean does not, however, lead to the importance of global ocean effect, since the other oceans may cancel out the Pacific contribution. Nevertheless, we think that the potential importance of the ocean as excitation source of CW is unequivocally illustrated since the realistic ocean data set is, to my knowledge, applied to the CW excitation problem for the first time.

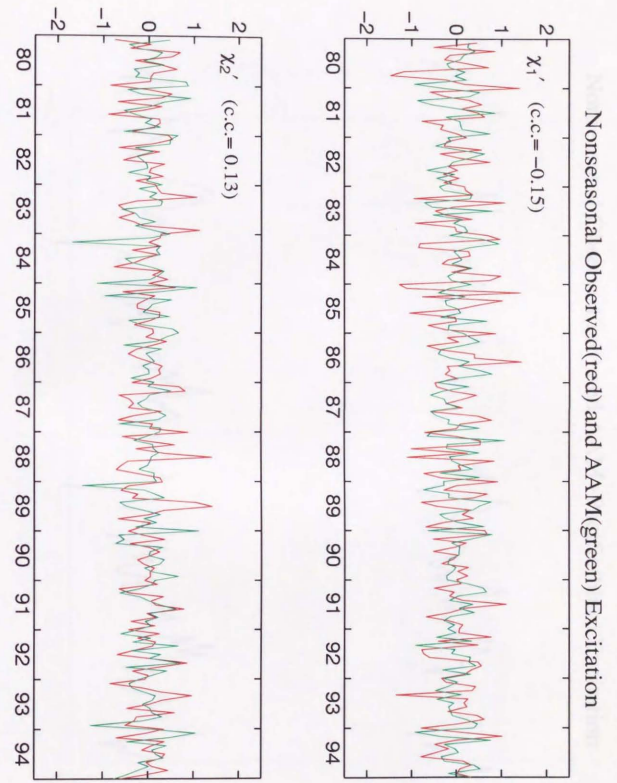

Figure 6.1: Vertical unit is 10^{-7} rad. Excitations shown above are based on modified coordinate axes.

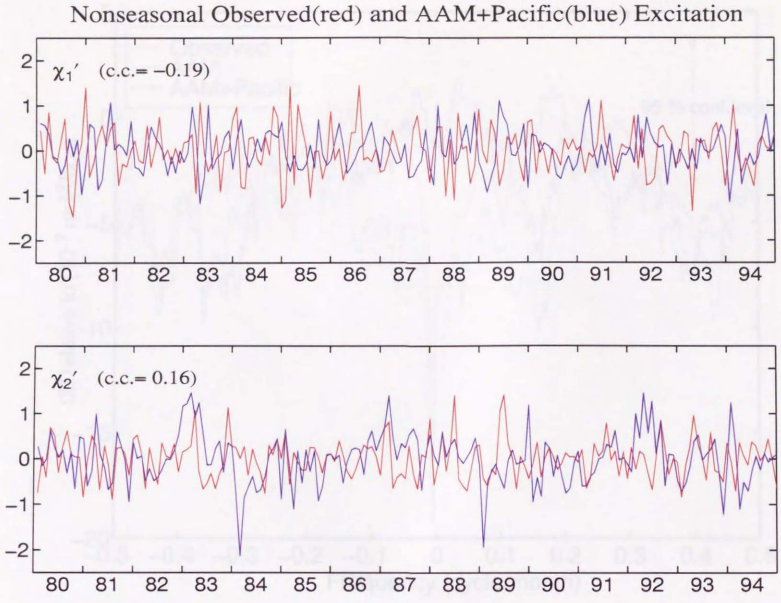

Figure 6.2: Vertical unit is 10^{-7} rad. Excitations shown above are based on modified coordinate axes.

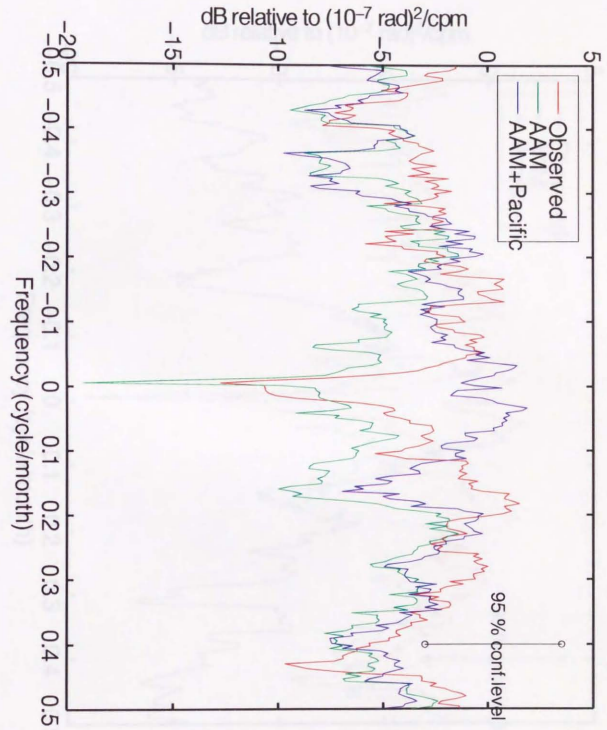

Figure 6.3: Power spectrum estimates for nonseasonal excitations. Red for Observed, Green for NCEP AAM, and Blue for NCEP AAM plus Pacific Ocean.

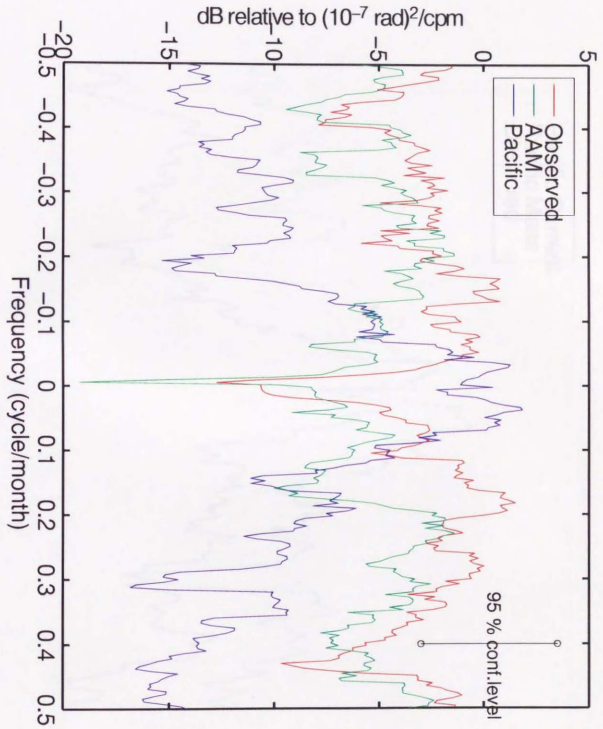

Figure 6.4: Power spectrum estimates for nonseasonal excitations.

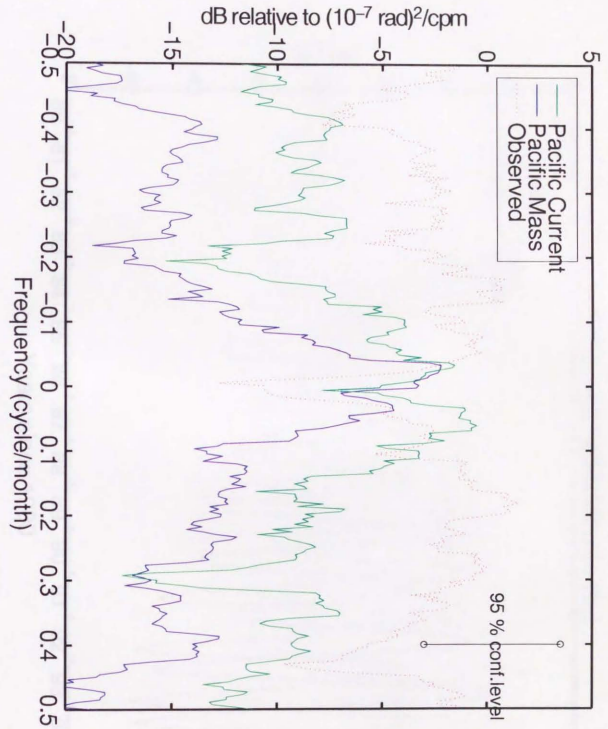

Figure 6.5: Power spectrum estimates for nonseasonal excitations.

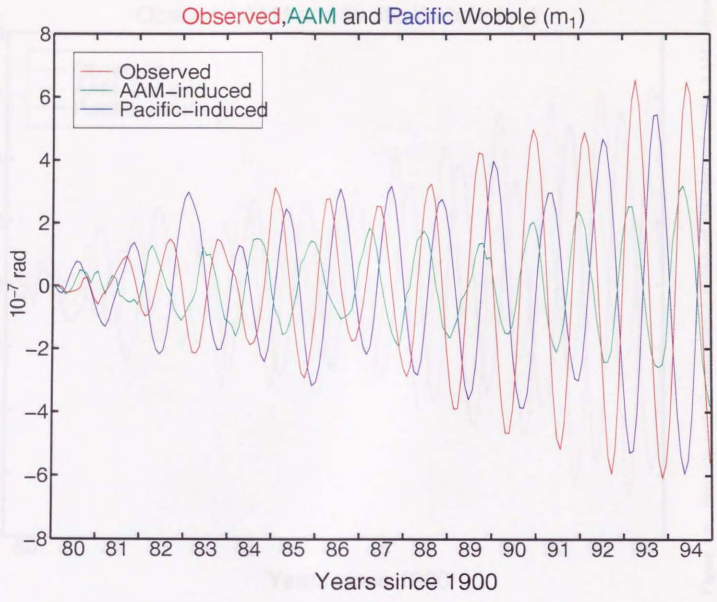
Observed,AAM and Pacific Wobble (m_1)
Observed
AAM–induced
Pacific–induced
10^{-7} rad
8
6
4
2
0
−2
−4
−6
−8
80 81 82 83 84 85 86 87 88 89 90 91 92 93 94
Years since 1900

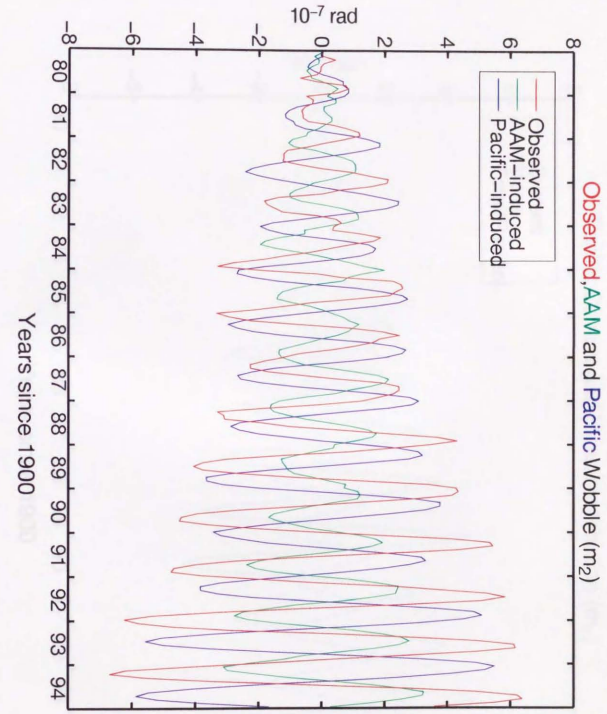

Figure 6.6: Recently excited non-seasonal wobble of the *observed* (red), AAM–induced (green), and Pacific Ocean–induced (blue) wobbles, where the Chandler period and Q–value are 434.0 days and 100, respectively. (a) m_1 (b) m_2 component.

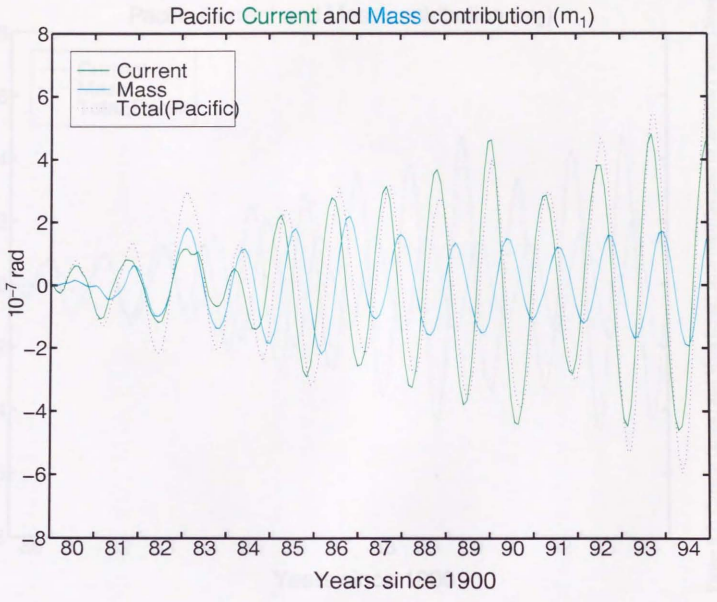
Pacific Current and Mass contribution (m_1)
Current
Mass
Total(Pacific)
10^{-7} rad
8
6
4
2
0
−2
−4
−6
−8
80 81 82 83 84 85 86 87 88 89 90 91 92 93 94
Years since 1900

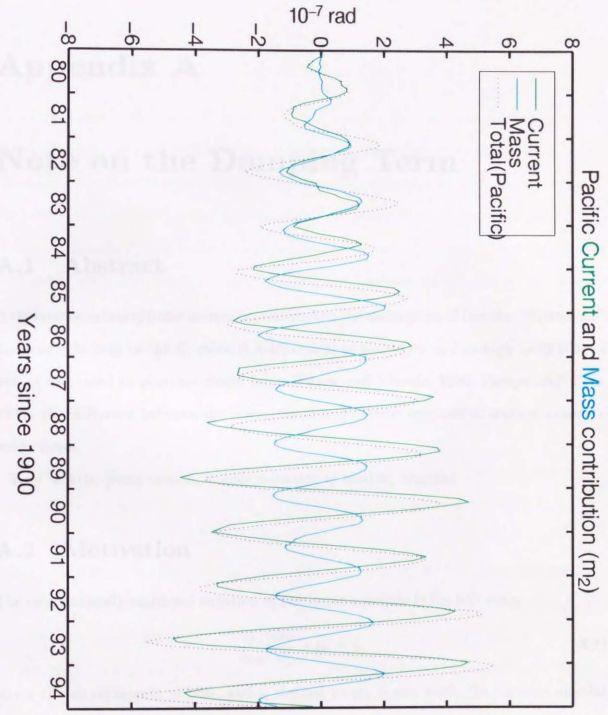

Figure 6.7: Current (green) and Mass (cyan) term contributions to the total Pacific Ocean–induced wobble. (a) m_1 (b) m_2 component.